Prague, Sptember 2024

ARCHITECTED MATERIALS IMPLEMENTED WITH UNSTABLE STRUCTURAL ELEMENTS

Davide Bigoni

University of Trento

Supported from ERC-ADG-2021-101052956-BEYOND

Department of Civil, Env. & Mechanical Engineering - University of Trento, Italy

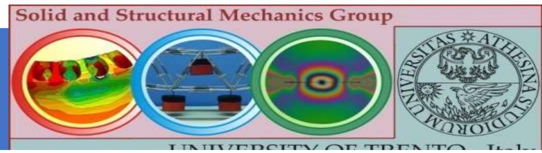

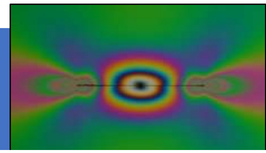

Elastic rods and nonlinear solids evidencing new effects

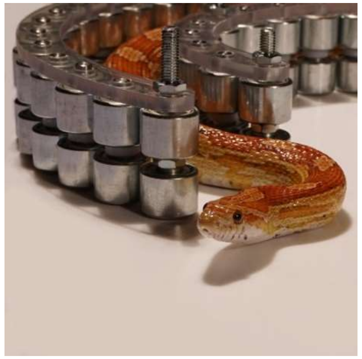

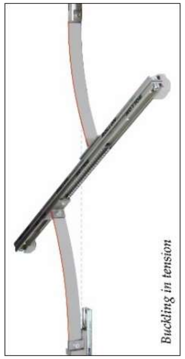

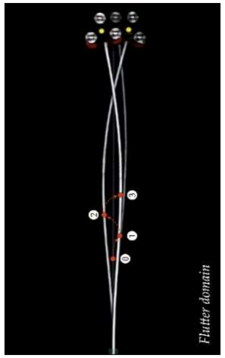

Configurational forces/Penetrating blade/Torsional gun/ Dripping of an elastic rod/Fluttering rods/
S-shaped constraints/Elastic snaking/Elastica catapult/Tensile buckling/Elastica arm scale

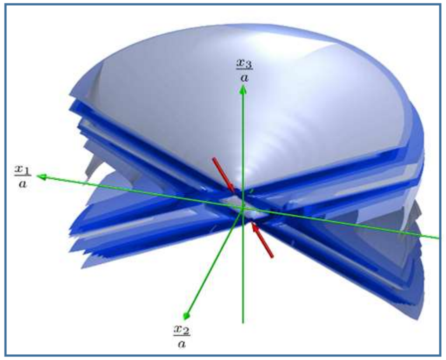

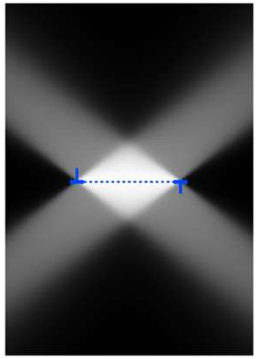

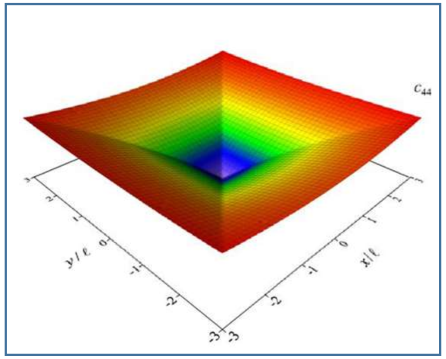

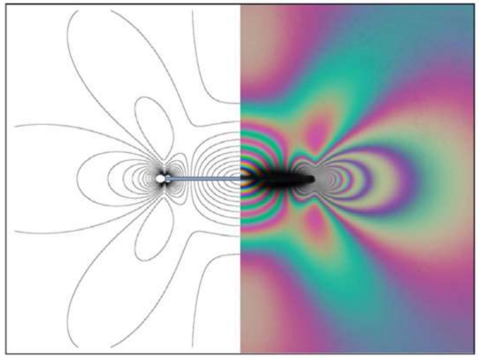

Perturbative approach to shear bands/Cones of localized deformation/Folding of a continuum/
Rigid line inclusion/Shear band patterns/Dynamics & shear bands/Flutter of a solid

Solids and Structures @ UniTn: the research team

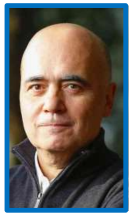
D. Bigoni
(Trento)


A. Cazzolli
(Trento)


F. Dal Corso
(Trento)


O. Kirillov
(Northumbria)


M. Tommasini
(Trento)


D. Misseroni
(Trento)


G. Noselli
(SISSA)


G. Bordiga
(Harvard)

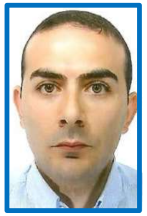
L. Cabras
(Brescia)


A. Piccolroaz
(Trento)


F. Bosi
(UCL)


C. Armanini
(New York Univ.)


P. Koutsogiannakis
(Trento)


M. Bacca
(UBC)

Time

2019 2018 2016 2014 2011

Configurational structural mechanics

Eshelby (1965) introduced the concept of configurational force to describe the motion of defects in solids through a release of energy

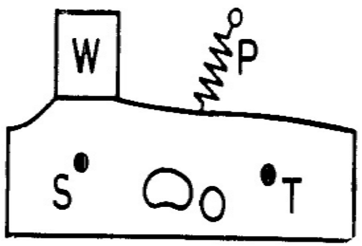

Total potential energy $\mathcal{V}$

Defect position α_i

Configurational force $F_i^c = -\dfrac{\partial \mathcal{V}}{\partial \alpha_i}$

In similar vein, we have extended the concept to structural mechanics

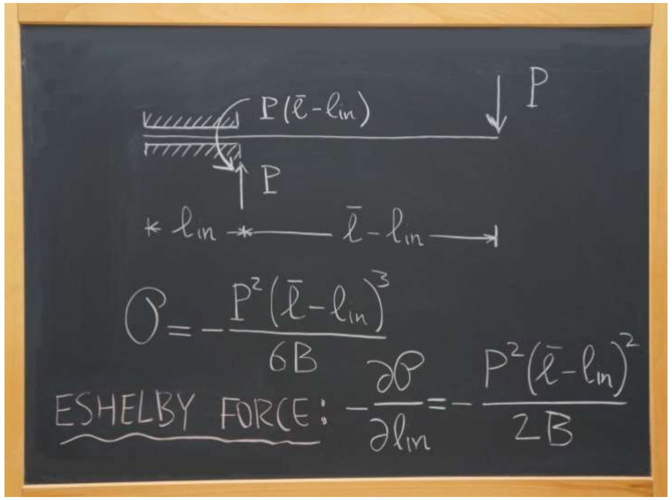

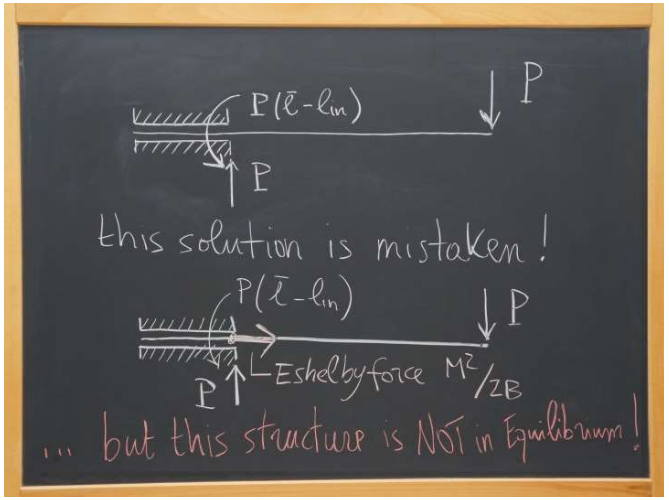

Configurational axial force

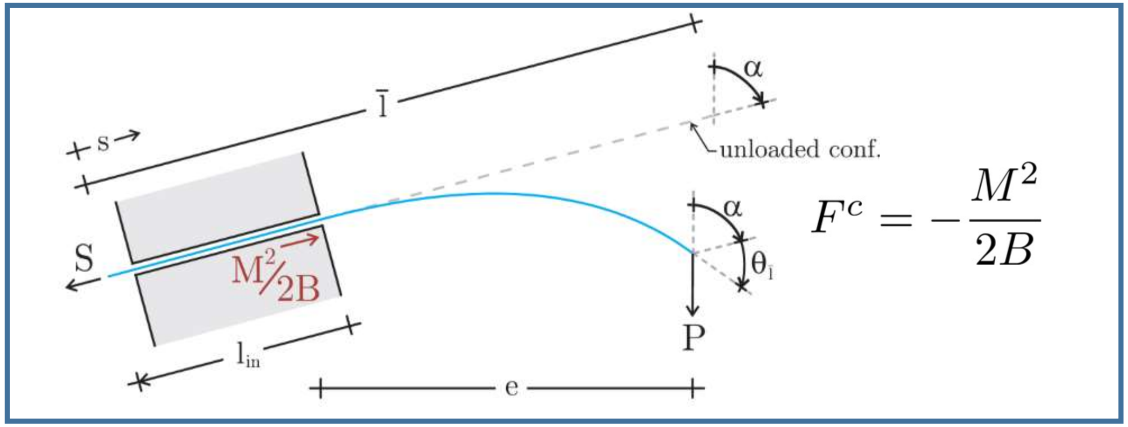

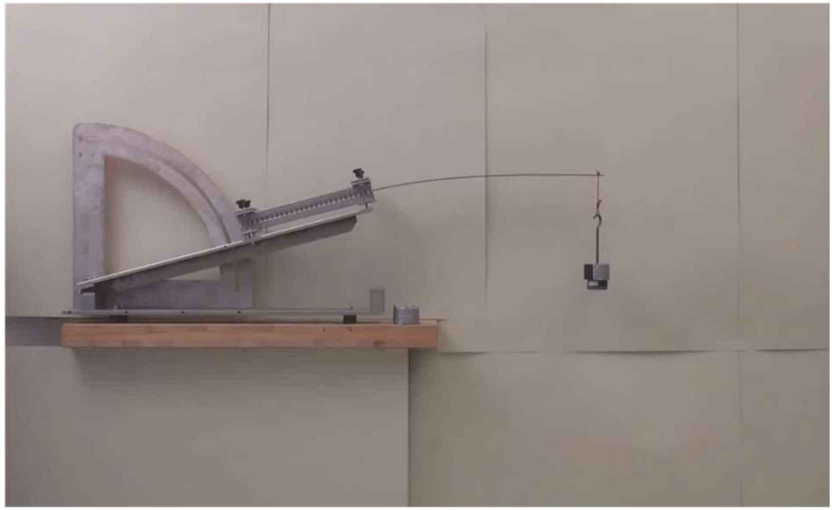

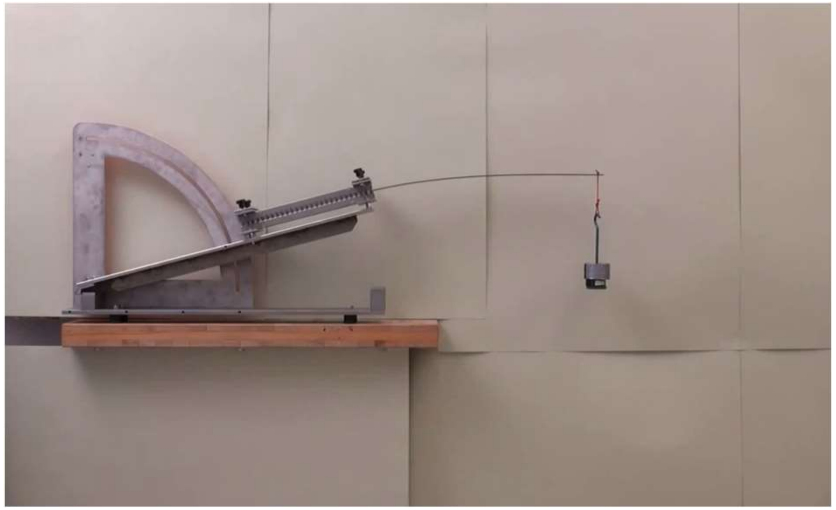

Free fall does not occur in a sort of inverted Kapitza pendulum

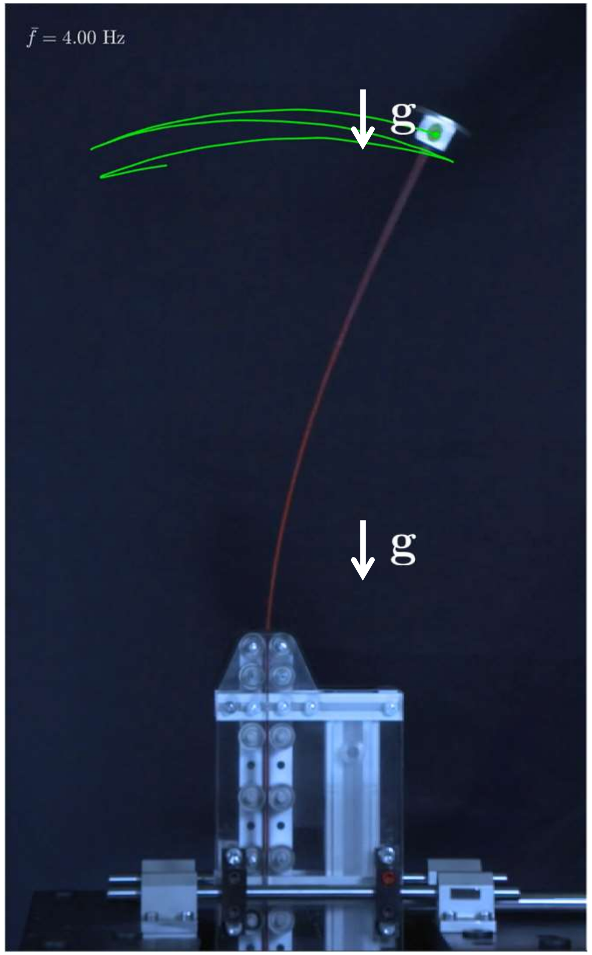

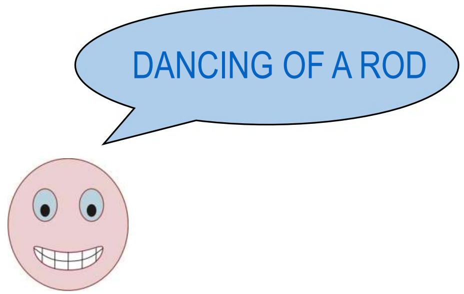

The dynamic ‘dance’: theory vs experiment

Experiment

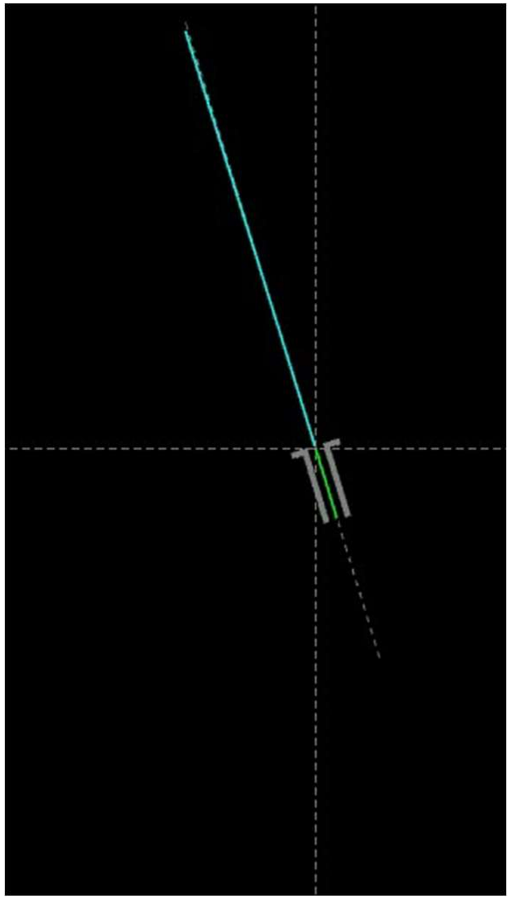

Simulation

Another configurational force: snake locomotion

Snakes have only 4 ways of moving around!

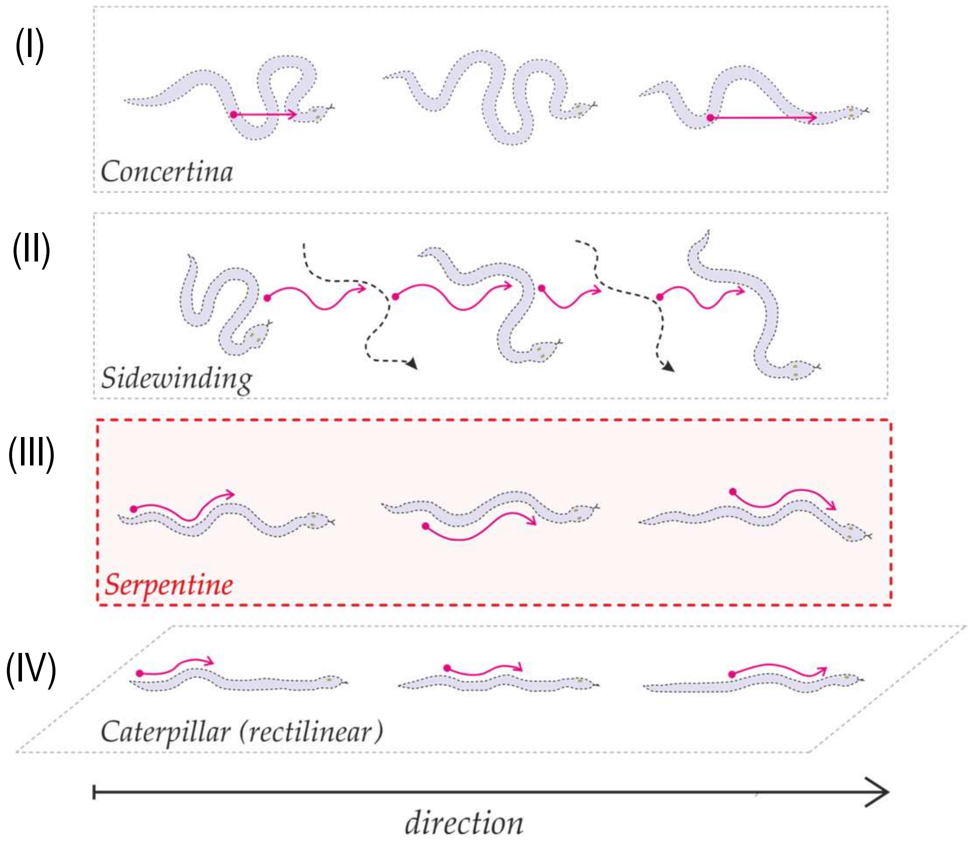

...serpentine locomotion!

Elastica constrained in a smooth and frictionless channel

Elastic flexural energy :

$$\mathcal{E}(\xi(t)) = \frac{1}{2}\int_0^l B(s)\,\chi^2(\xi(t)+s)\,ds$$

Kinetic energy:

$$\mathcal{T}(\dot{\xi}(t)) = \frac{1}{2}\mu\left[\dot{\xi}(t)\right]^2, \qquad \mu = \int_0^l \gamma(s)ds$$

Total potential energy

$$\mathcal{V}(t) = \mathcal{E}(t) + \mathcal{T}(t)$$

The channel is frictionless:

$$\dot{\mathcal{V}}(t) = \dot{\mathcal{E}}(t) + \dot{\mathcal{T}}(t) = \left[\frac{\partial \mathcal{E}(\xi)}{\partial \xi} + \mu\ddot{\xi}\right]\dot{\xi}(t) = 0$$

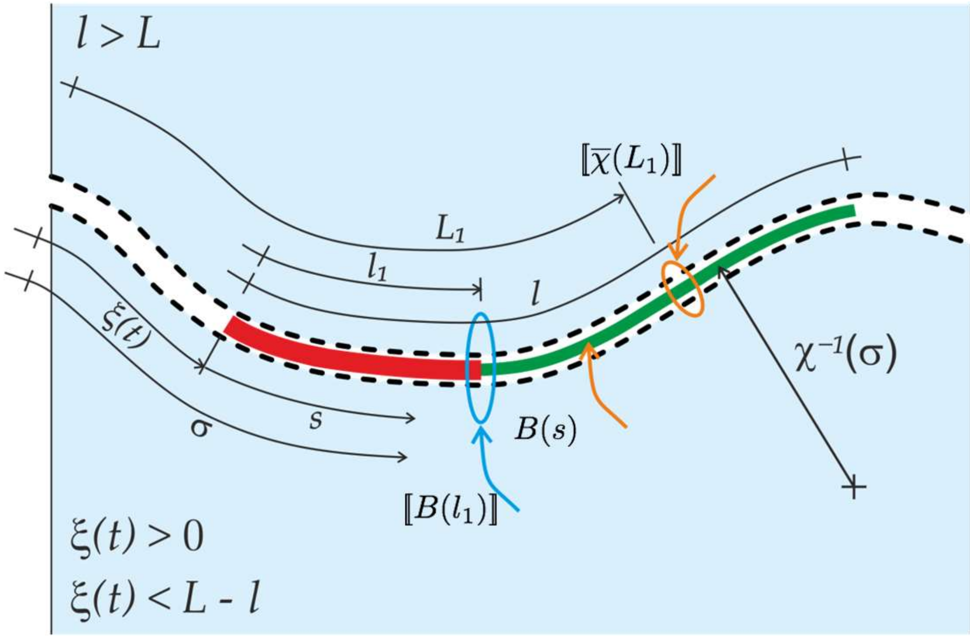

Propulsive force

$$P = \left(1 + \frac{\partial s_1(\xi)}{\partial \xi}\right)\frac{B(s_1(\xi))\overline{\chi}^2\,(\xi + s_1(\xi))}{2} - \left(1 + \frac{\partial s_2(\xi)}{\partial \xi}\right)\frac{B(s_2(\xi))\overline{\chi}^2\,(\xi + s_2(\xi))}{2}$$

Experiments on the snaking rod

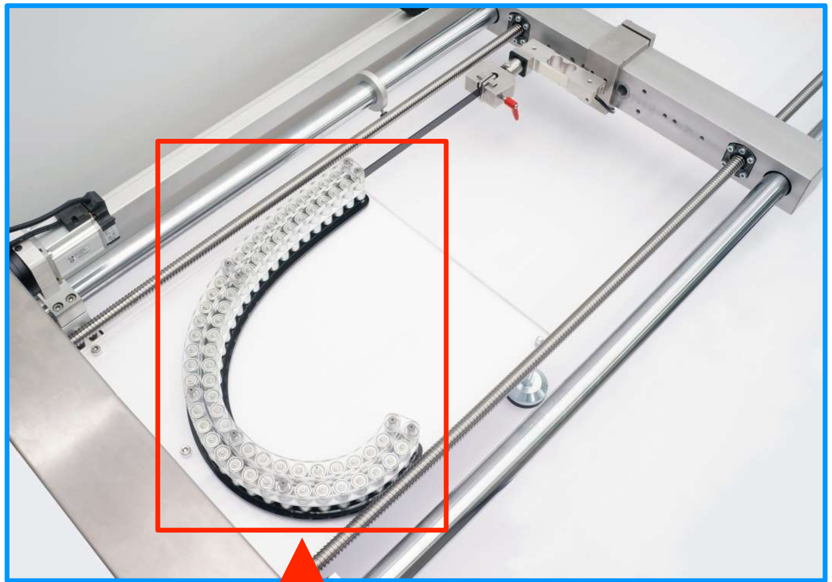

Euler spiral (clothoid):

...curve whose curvature changes linearly with its curve length!

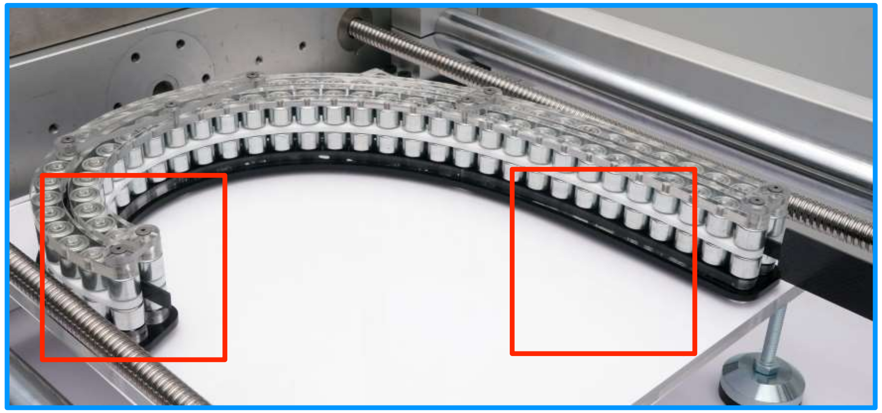

Qualitative proof of the propulsion

Configurational propulsive force vs experiments

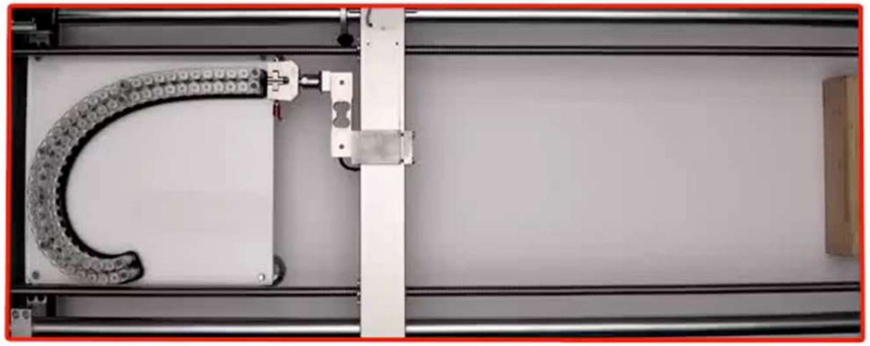

5x Fast Motion

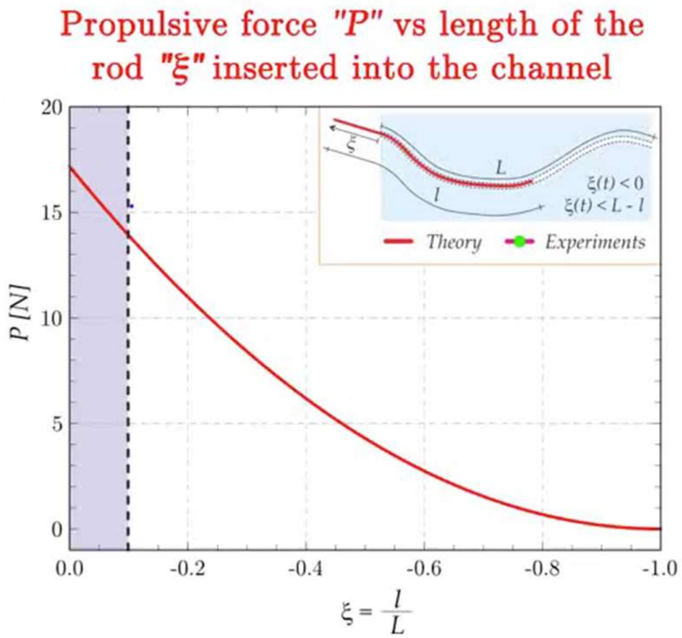

Tensile buckling: inspired from shear bands

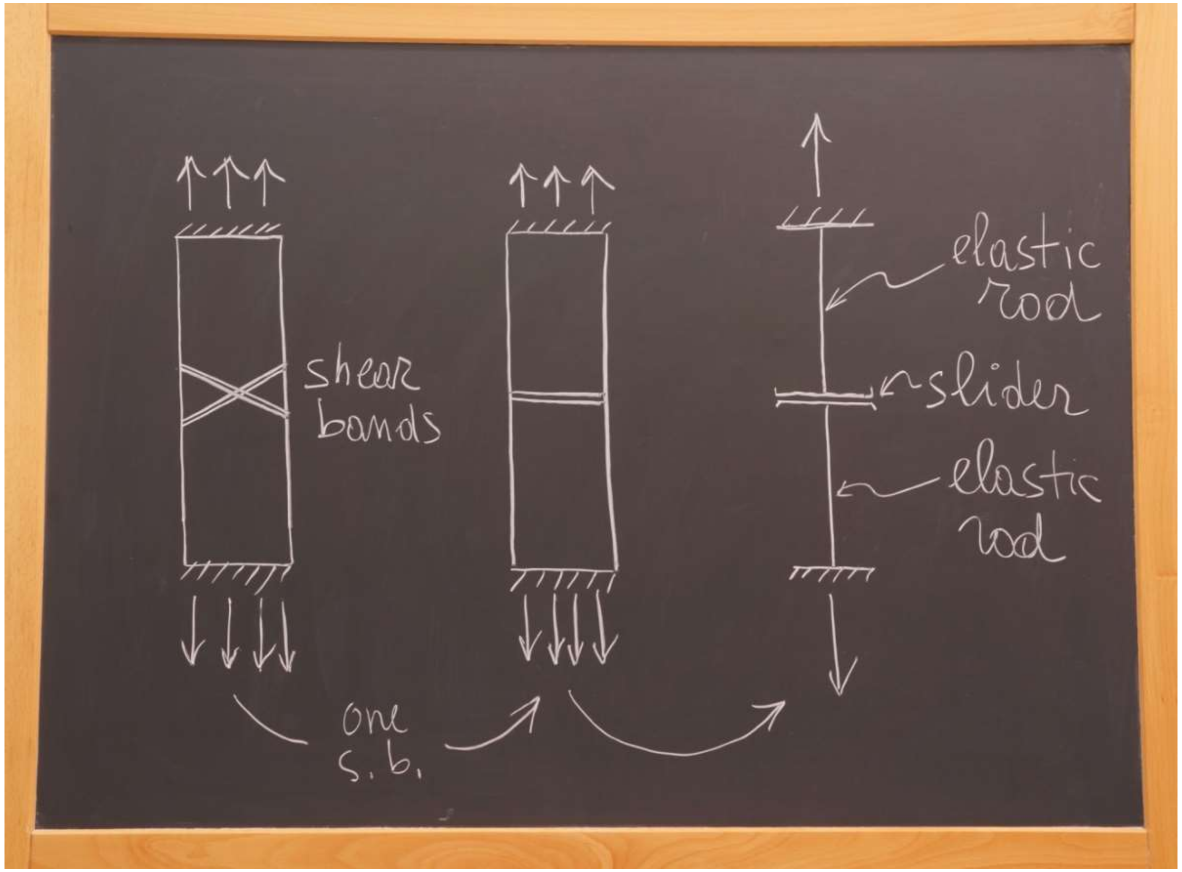

Tensile buckling

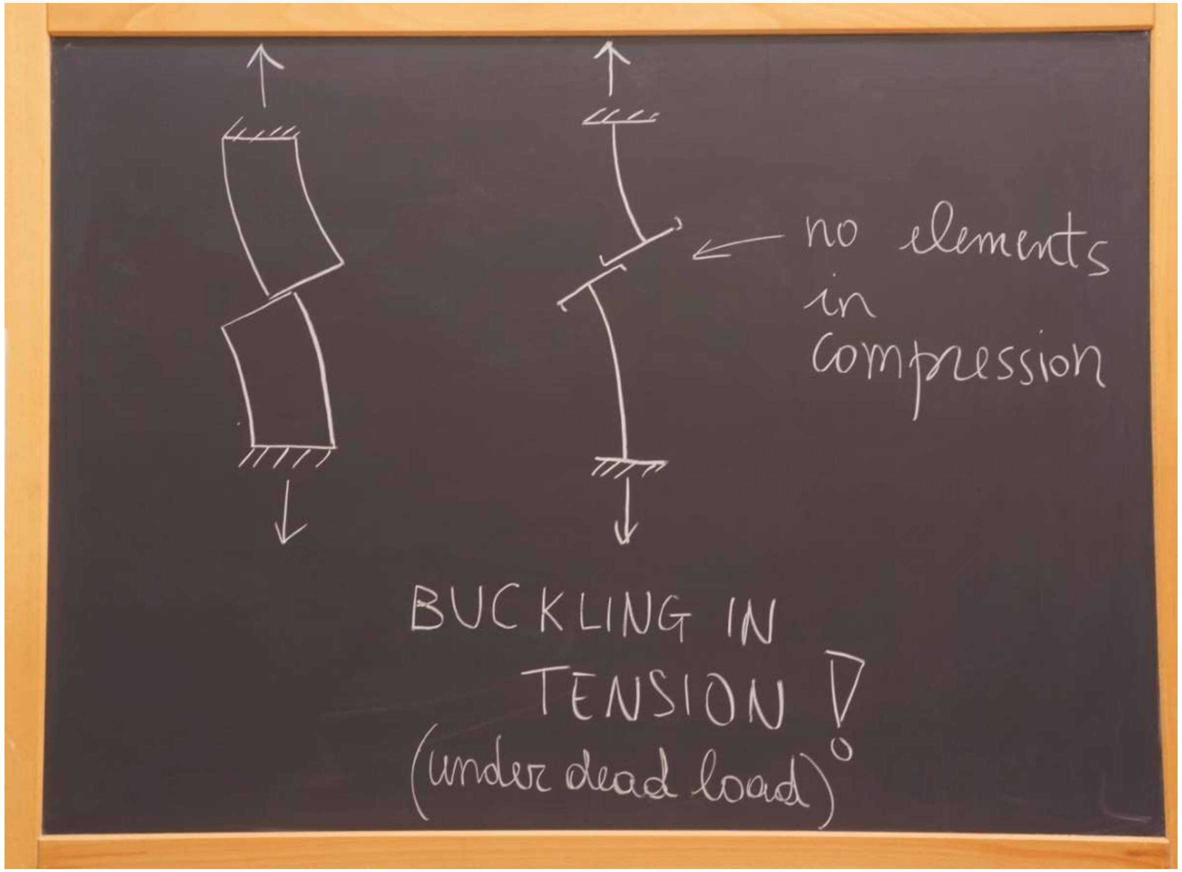

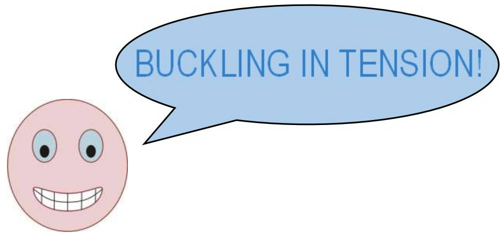

Fully nonlinear analysis confirms buckling

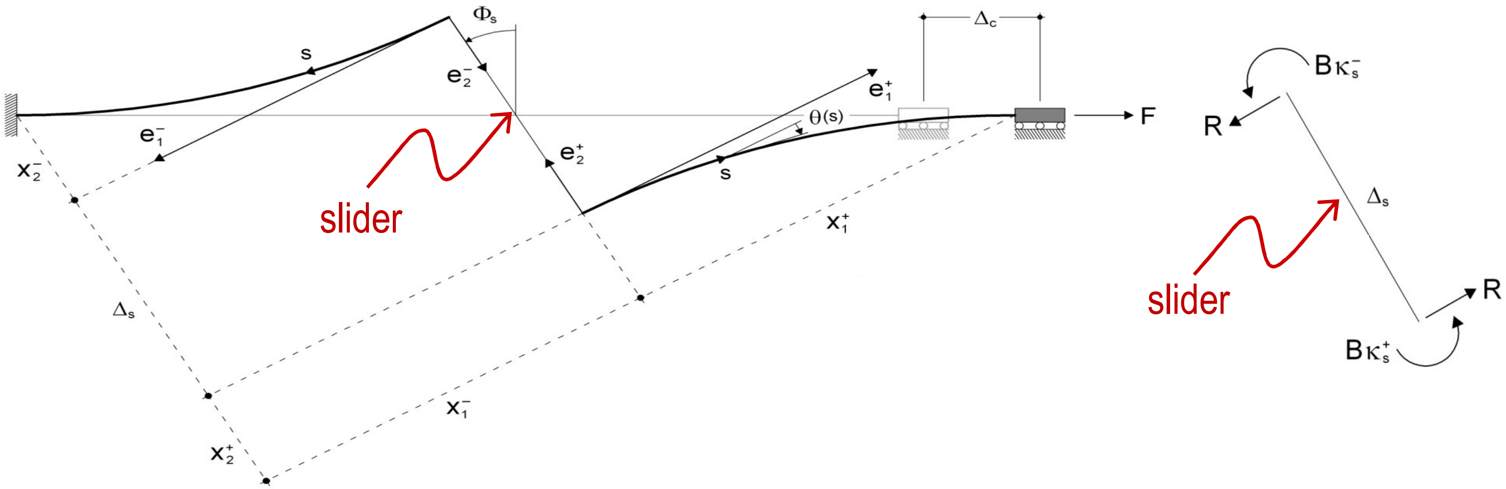

1) Kinematic compatibility

$$\left[x_1^-(l^-) + x_1^+(l^+)\right] \tan\Phi_s + x_2^-(l^-) + x_2^+(l^+) + \Delta_s = 0$$

2) Force orthogonal to the slider

$$R = \frac{F}{\cos\Phi_s}$$

3) Equilibrium of the slider

$$\kappa_s^- + \kappa_s^+ = \frac{R}{B}\Delta_s$$

4) Elastica for both rods

$$\frac{d^2\theta}{ds^2} - \frac{R}{B}\sin\theta = 0$$

... and experiments also show tensile buckling

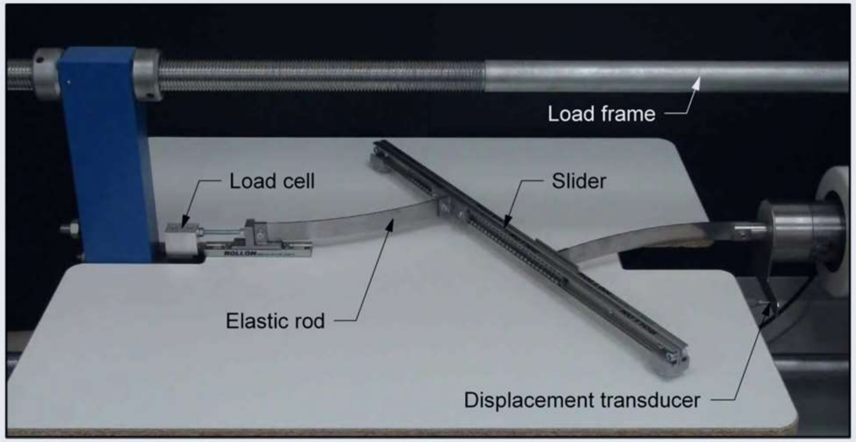

1 DoF structure with 2 buckling loads: in tension and in compression

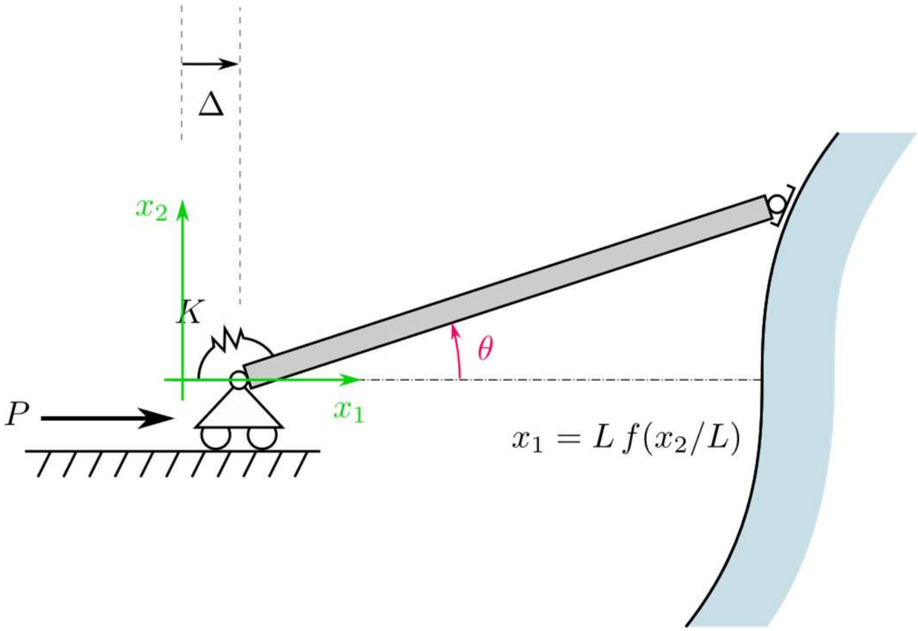

Compression

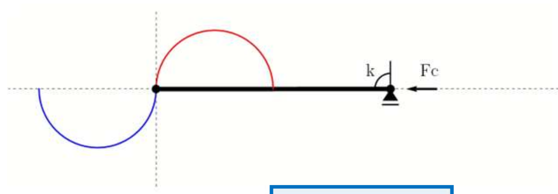

$$\boxed{F_c = -\frac{K}{5l}}$$

Compressive buckling

Tension

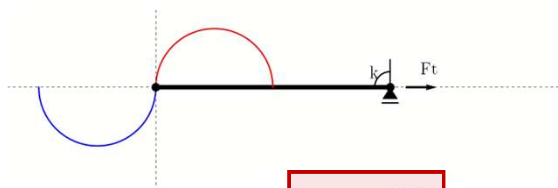

$$\boxed{F_t = \frac{K}{3l}}$$

Tensile buckling

Flutter: the Ziegler double pendulum

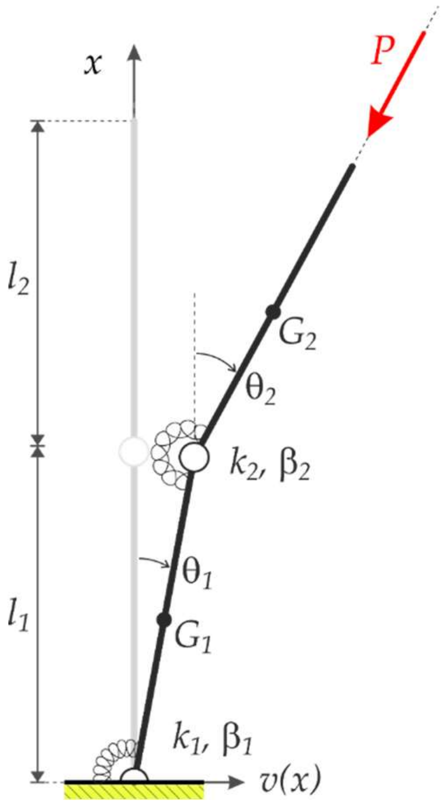

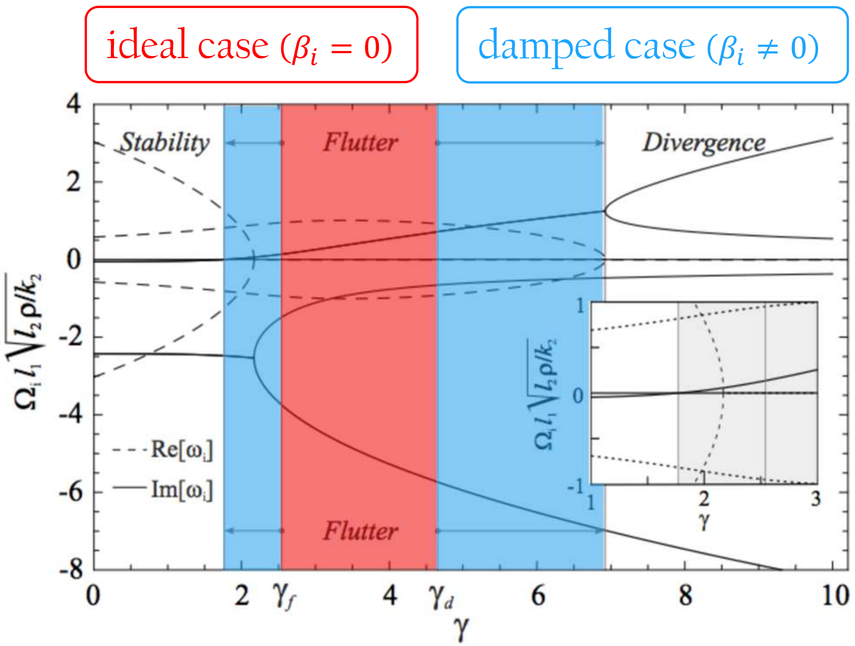

$$\omega = \Omega l_1 \sqrt{\frac{\rho l_2}{k_2}} \qquad \gamma = \frac{P\, l_1}{k_2}$$

$$\gamma_{f,d} = \frac{k + (1+\lambda)^3 \pm \lambda\sqrt{\kappa(3+4\lambda)}}{1 + 3/2\lambda}, \quad \lambda = \frac{l_1}{l_2}, \quad \kappa = \frac{\kappa_1}{\kappa_2}$$

1st Problem

How to provide the follower force?

Professor Warner T. Koiter:

"I propose the elimination of the abstraction of follower forces as external loads from the physical and engineering literature on elastic stability"

Two important attempts:

G. Herrmann et al. (1966) and Y. Sugiyama et al. (1995)
- by a fluid flowing through a nozzle
- by a solid rocket motor mounted on the top of the structure

Can we do better?

The first experimental setup

The load P is proportional to the reaction R provided via a lever principle hanging the dead load W (Bigoni & Noselli, JMPS, 2012)

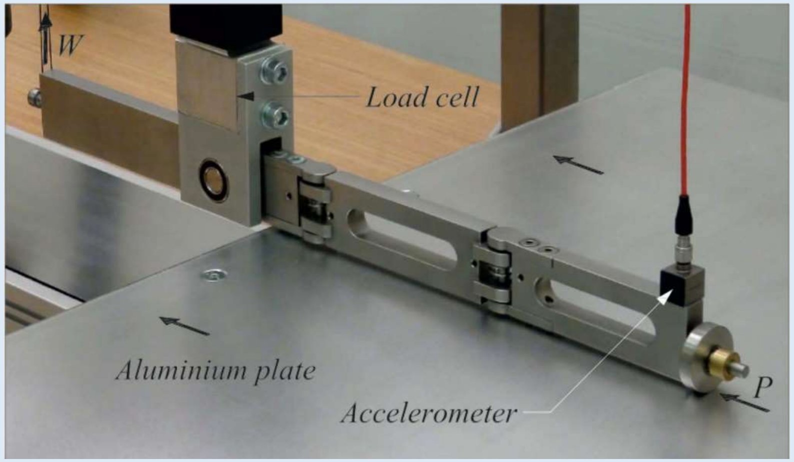

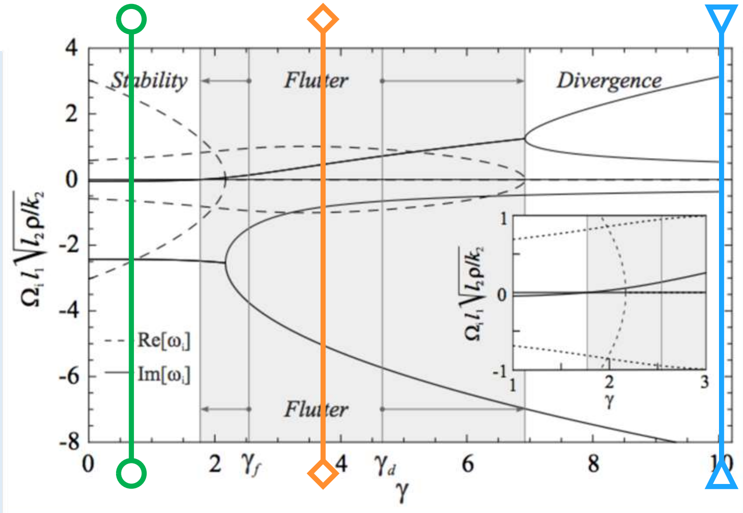

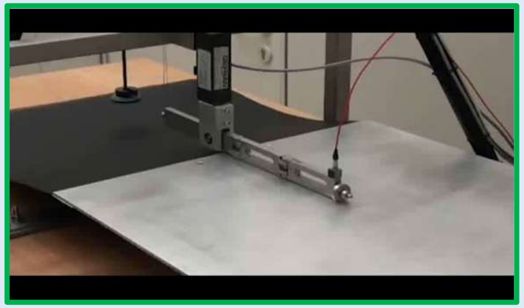

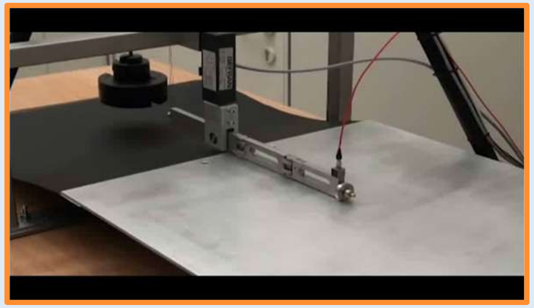

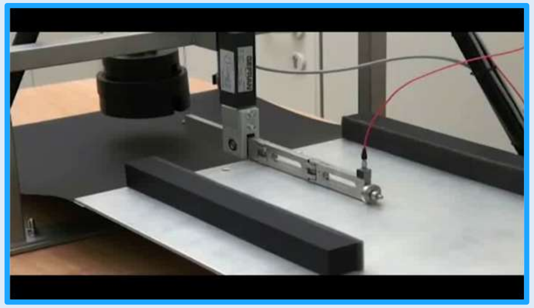

○ Stability: γ=0.622

◇ Flutter: γ=3.606

△ Divergence: γ=10.017

From a discrete to a continuous system

Internal/external dampings (Detinko, 2003)

Linearized differential equation of motion

$$EJv''''(x,t) + E^*J\dot{v}''''(x,t) + Pv''(x,t) + \\ + K\dot{v}(x,t) + m\ddot{v}(x,t) = 0$$

Boundary conditions

$$\begin{cases} v(0,t) = v'(0,t) = 0 \\ \mathcal{M}(l,t) = -J[Ev''(l,t) - E^*\dot{v}''(l,t)] = 0 \\ \mathcal{T}(l,t) = -J[Ev'''(l,t) - E^*\dot{v}'''(l,t)] = P\bar{\chi}v'(l,t) - M\ddot{v}(l,t) \end{cases}$$

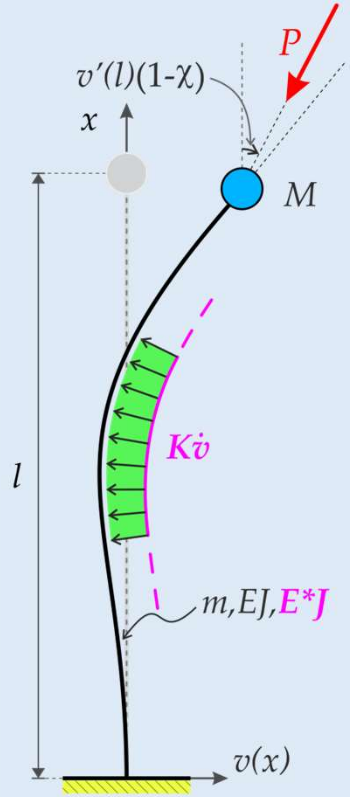

Experiment vs Simulations

Record of some experiments and comparison with the numerical simulations

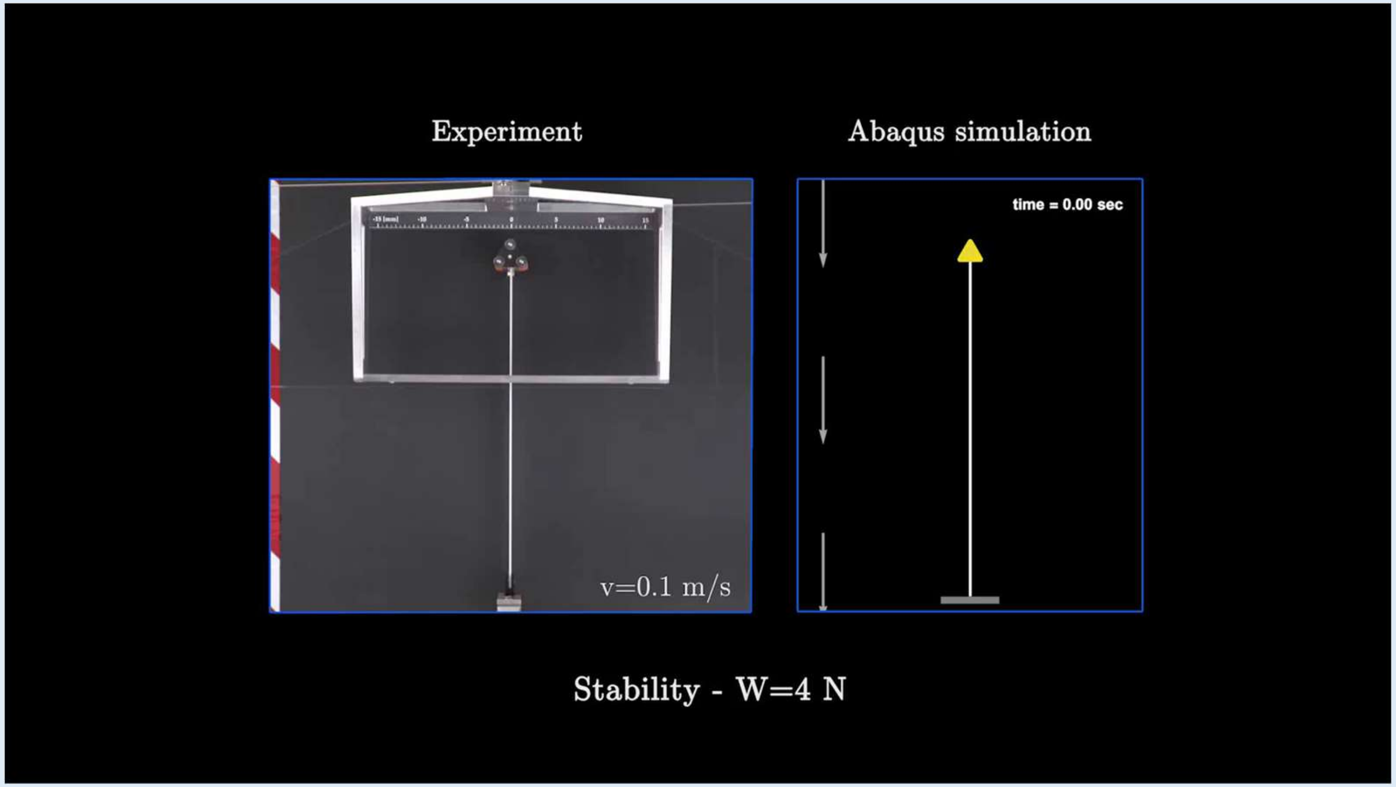

The experimental results

Flutter and the divergence thresholds

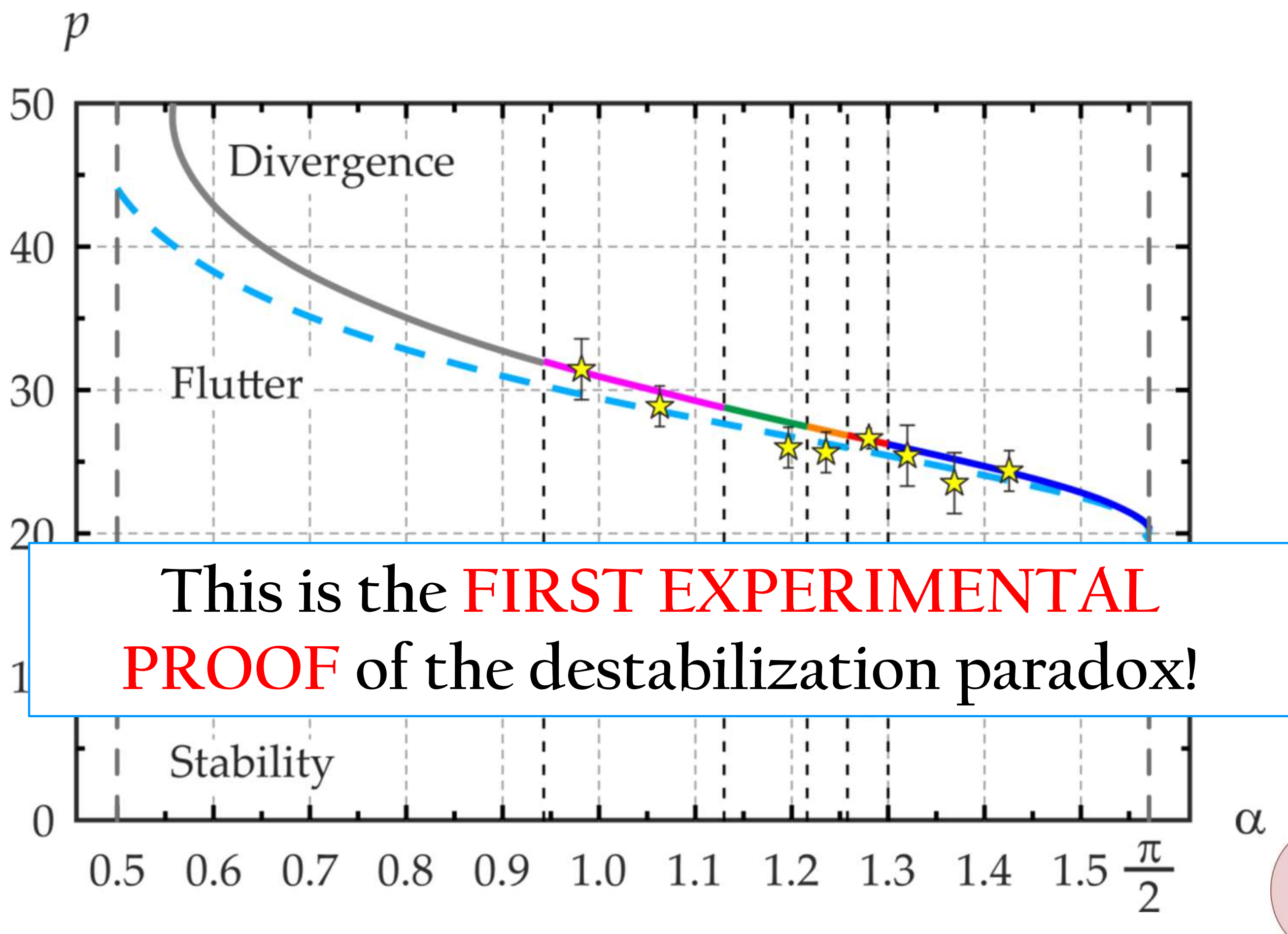

This is the FIRST EXPERIMENTAL PROOF of the destabilization paradox!

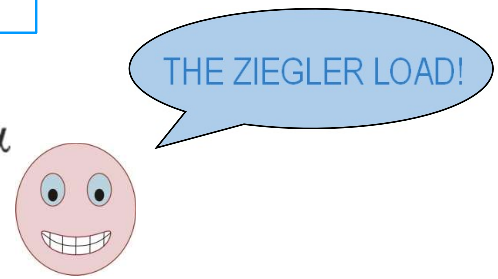

The Reut column

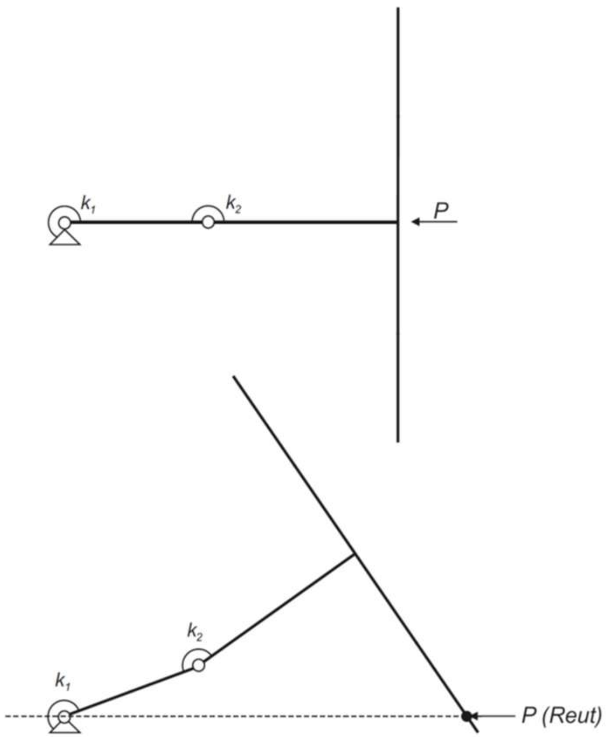

The force P always acts along a line

Problem: how to provide the Reut's load?

How to provide the follower force?

Always the same problem!

Two important attempts:

G. Herrmann et al. (1966) and Y. Sugiyama et al. (1995)
- an air jet impinging the structure

Can we do better?

The Reut column: flutter instability experiment

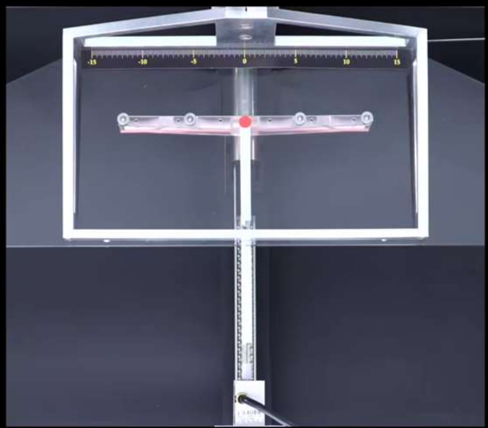

Flutter - P=15 N, v_p=20 mm/s

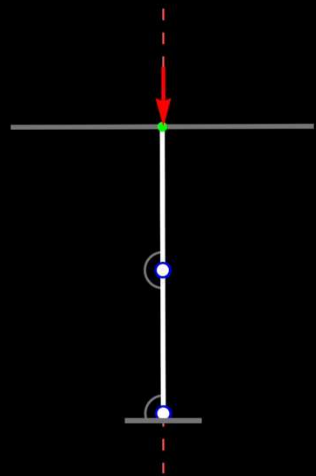

Flutter - P=15 N, v_p=20 mm/s

Another proof of the Ziegler paradox

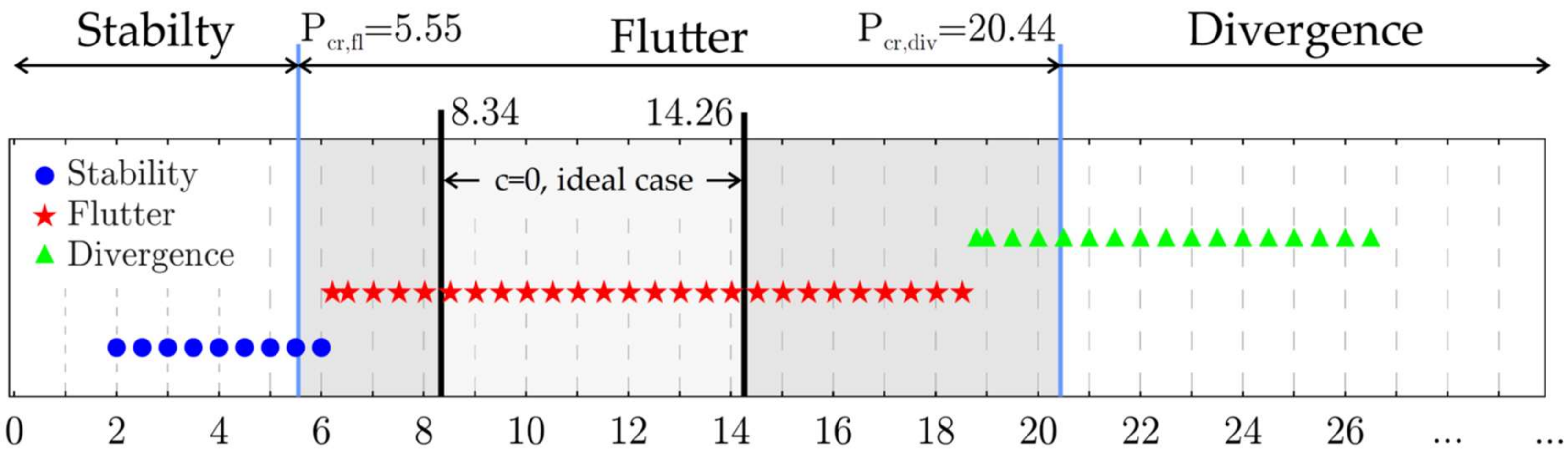

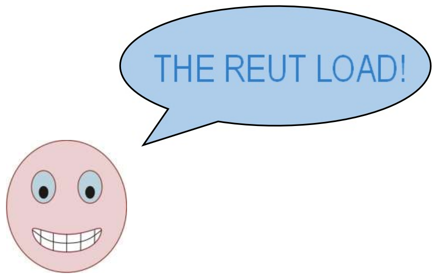

Is it possible to get rid of friction?

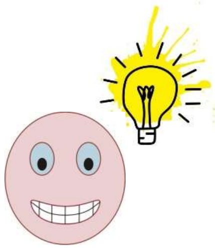

Non-holonomic constraints!

These constraints apply to the velocity, ***not*** to the position

For instance a wheel rolling without slip or a perfectly sliding skate

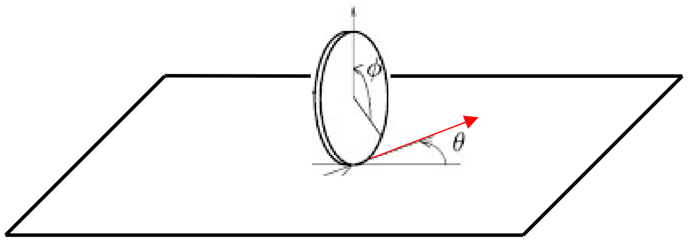

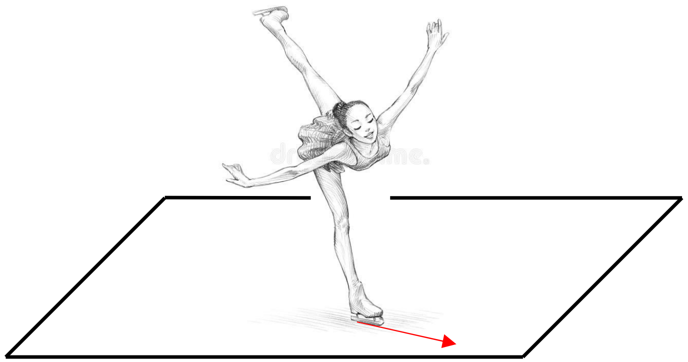

Flutter has been related to non-conservative loads

Elishakoff: ‘Bolotin felt –if my memory serves me well!– that it should be impossible to produce Beck’s column experiment via a conservative system of forces.’

Anderson and Done: ‘Sometimes, the creation of a force like [a follower force] in the laboratory presents awkward practical problems, and the simulation of this force wherever possible by a conservative force would be very convenient. However, because of the differing nature of the fundamental properties of the conservative and non-conservative systems, <u>the simulation could only work in a situation where the two systems behave in similar ways; that is when the conservative system is not operating in a regime of oscillatory instability. (The conservative system can not become dynamically instable since, by definition, it has no energy source from which to supply the extra kinetic energy involved in the instability)</u>.’

Koiter: ‘[...] it appears impossible to achieve any non-conservative loading conditions in the laboratory by purely mechanical means’, because ‘non-conservative external loads always require an external energy source, much as a fluid flow or an interaction with electro-dynamic phenomenon’.

Singer: ‘An example in the field of elastic stability of what Drucker referred to as playing useless games was presented by Koiter, in his 1985 Prandtl lecture, where he discussed the physical significance of instability due to non-conservative, purely configuration-dependent, external loads.’

... but non-holonomic constraints perserve conservation of energy!!

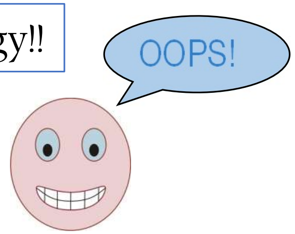

Loads are conservative

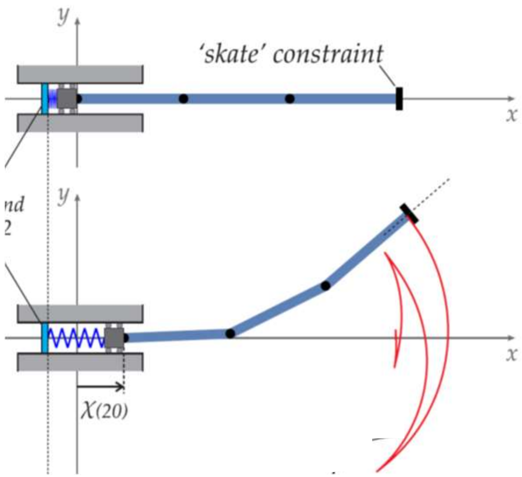

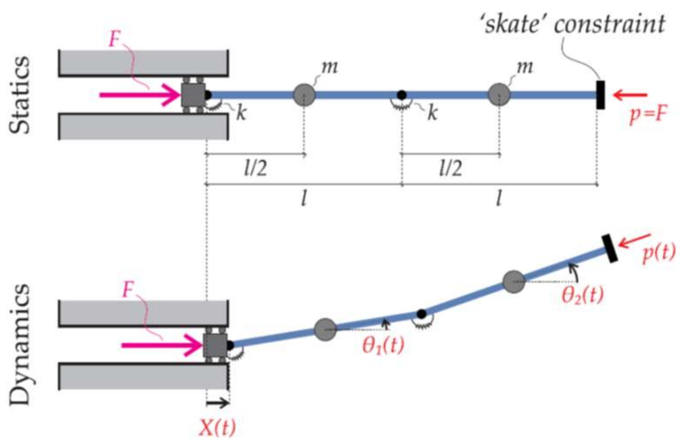

Flutter instability, Ziegler's paradox, Hopf bifurcation and limit cycle occur
for conservative systems!!!!

Loads through a dead force: viscoelastic system

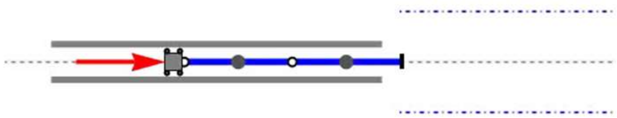

Skate
(Ziegler's type)

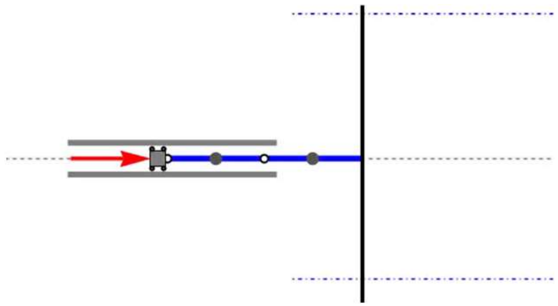

Violin bow
(Reut's type)

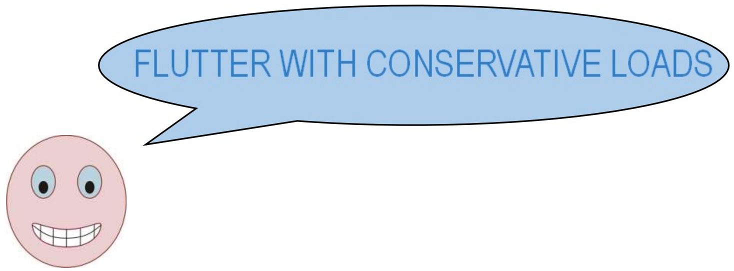

Two stable structures lead to an unstable compound structure

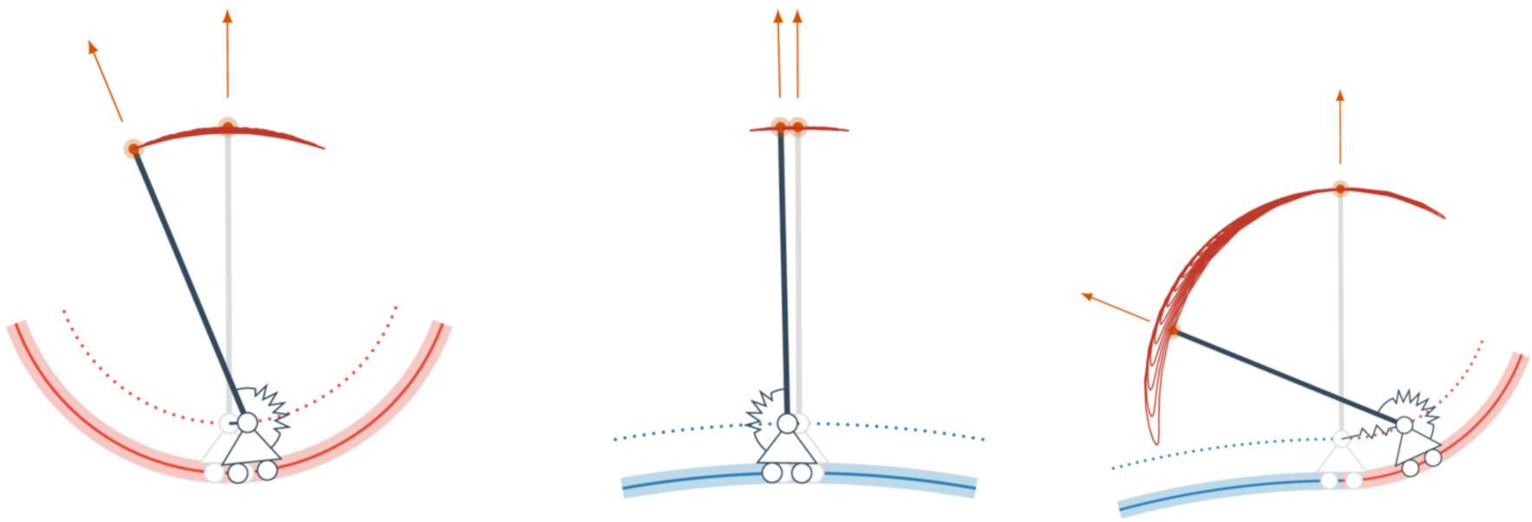

Stable | Stable | Unstable!

A stable 2 d.o.f. structure: video

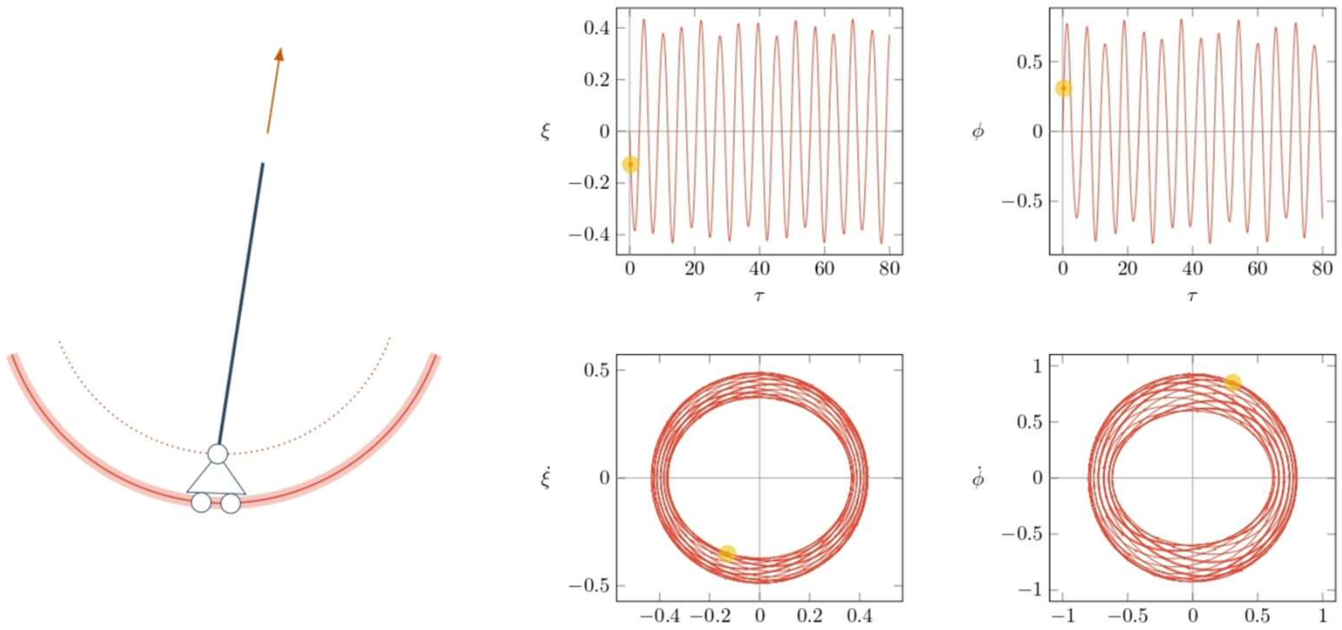

Another stable 2 d.o.f. structure: video

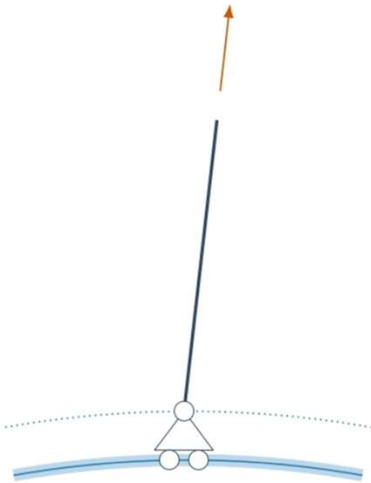

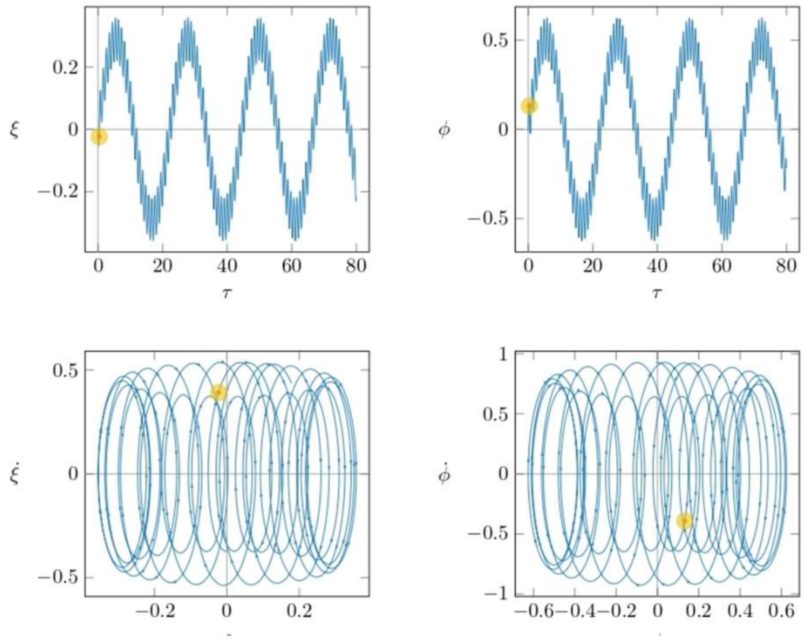

How to address the discontinuous problem?

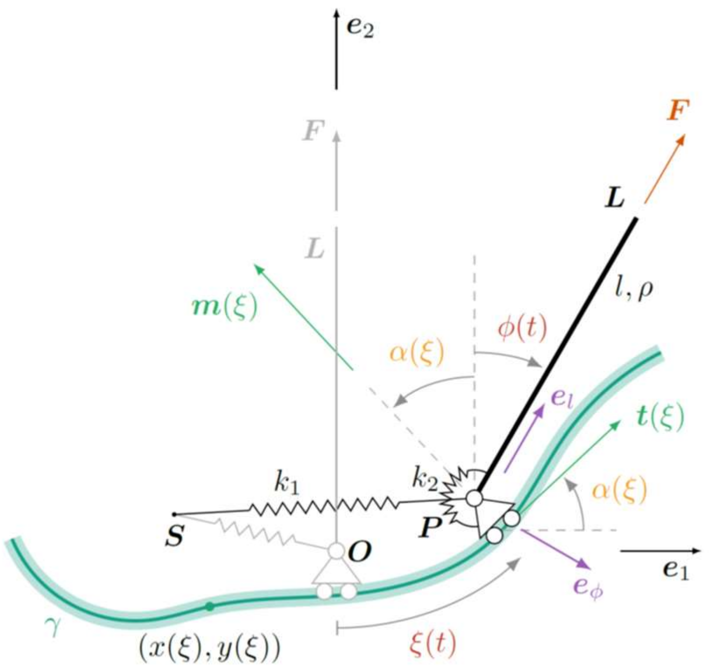

$$\rho\frac{l^2}{2}\ddot{\phi}x'(0) + [k_2\alpha' - Fx']_{\xi=0}\,\phi + \rho l\ddot{\xi}\left[x'^2 + y'^2\right]_{\xi=0}$$
$$+ \left[k_1\left(x''(x - x_S) + x'^2 + y''(y - y_S) + y'^2\right) - Fy'' + k_2\left(\alpha'^2 + \alpha\alpha''\right)\right]_{\xi=0}\xi$$
$$+ \left[k_1\left(x'(x - x_S) + y'(y - y_S)\right) - Fy' + k_2\alpha'\alpha\right]_{\xi=0} = 0,$$

$$\rho\frac{l^3}{3}\ddot{\phi} + k_2\phi + \rho\frac{l^2}{2}x'(0)\ddot{\xi} + k_2\alpha'(0)\xi + k_2\alpha(0) = 0.$$

$$\boldsymbol{K}^{\pm} = \begin{bmatrix} k_1 + \dfrac{k_2}{R_{\pm}^2} \mp \dfrac{k_1 y_s}{R_{\pm}} \mp \dfrac{F}{R_{\pm}} & \pm\dfrac{k_2}{R_{\pm}} - F \\ \pm\dfrac{k_2}{R_{\pm}} & k_2 \end{bmatrix}$$

$$\begin{cases} \boldsymbol{M}\ddot{\boldsymbol{q}}(t) + \boldsymbol{K}^{-}\boldsymbol{q}(t) = \boldsymbol{0}, & \xi < 0 \\ \boldsymbol{M}\ddot{\boldsymbol{q}}(t) + \boldsymbol{K}^{+}\boldsymbol{q}(t) = \boldsymbol{0}, & \xi > 0 \end{cases}$$

Linearized dynamics with a piecewise smooth constraint

Mechanical energy

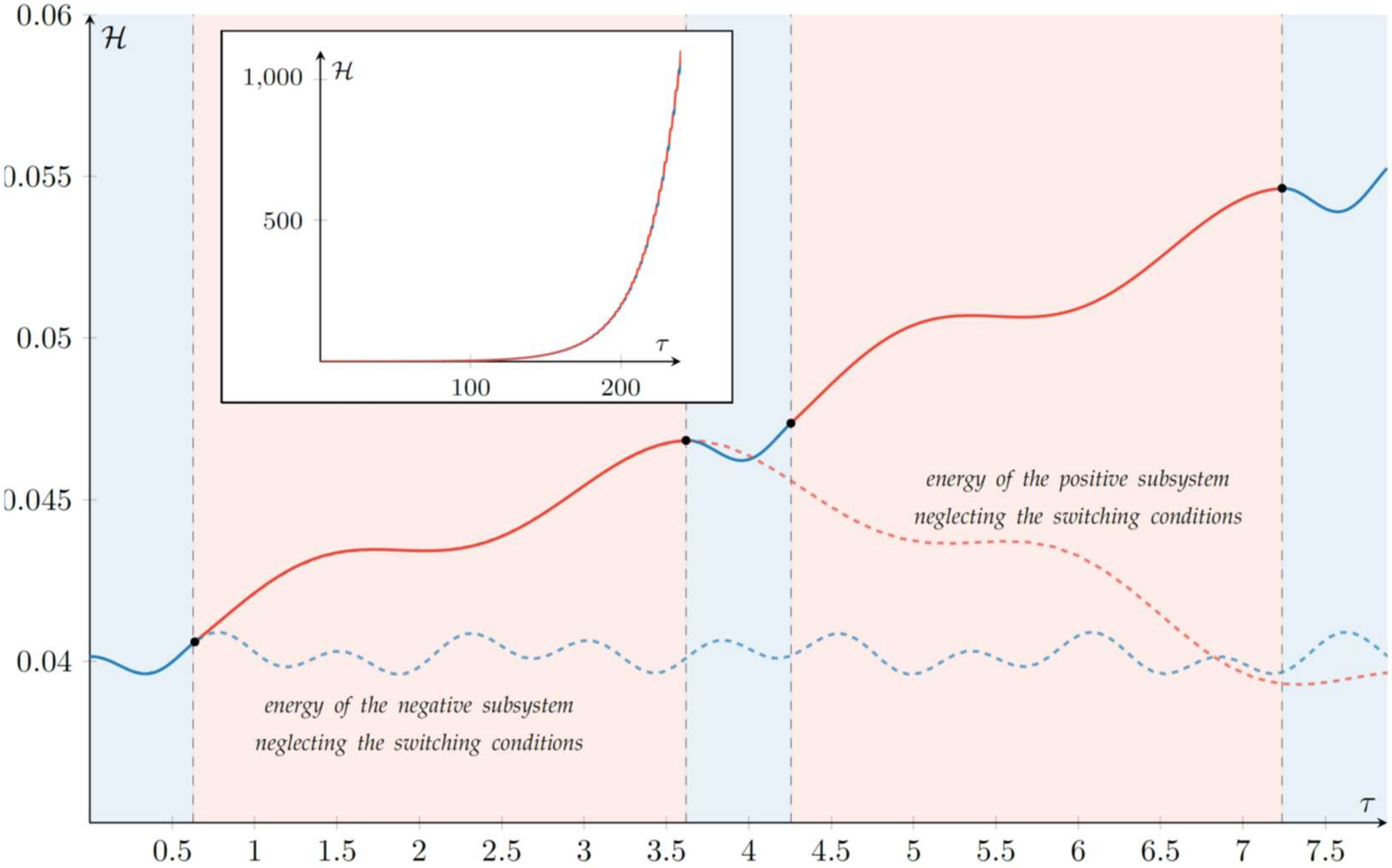

Instability for linearized equations

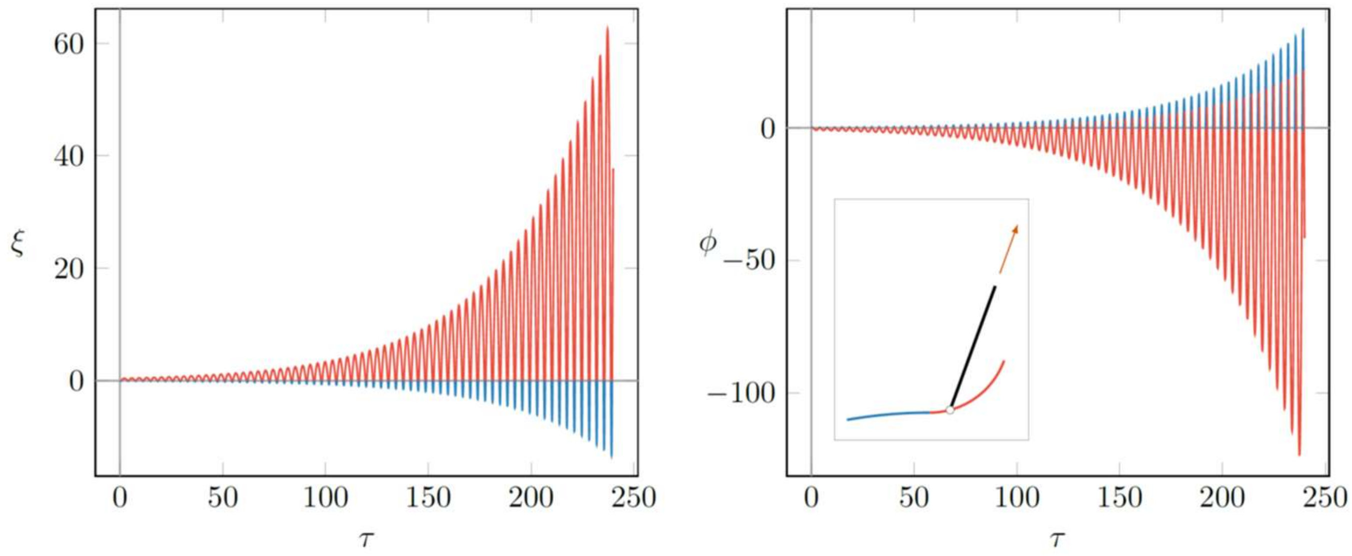

Instability in the nonlinear range

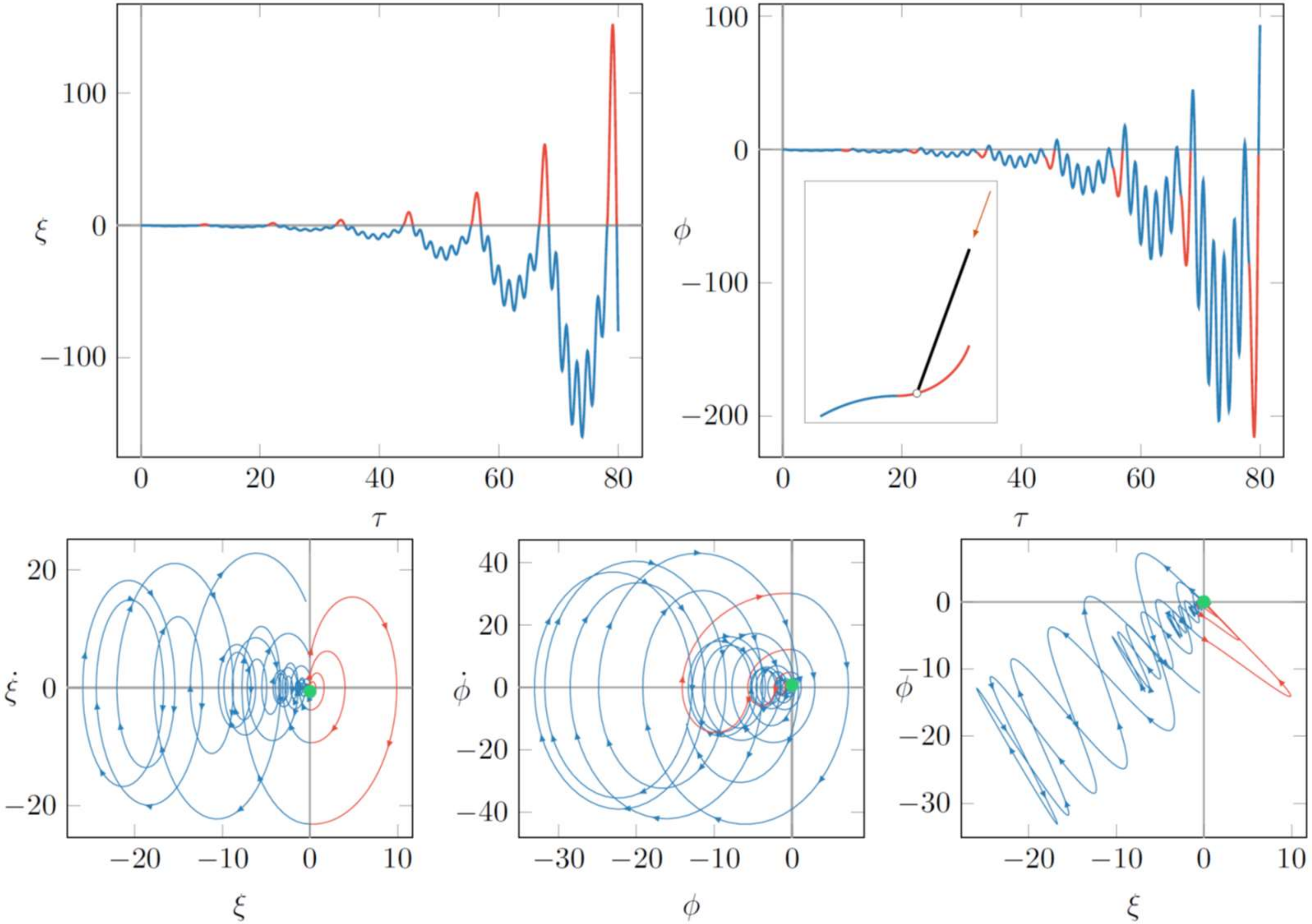

The instability of the compound structure

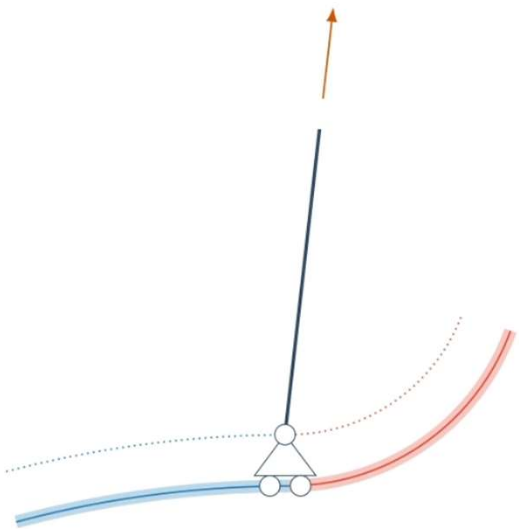

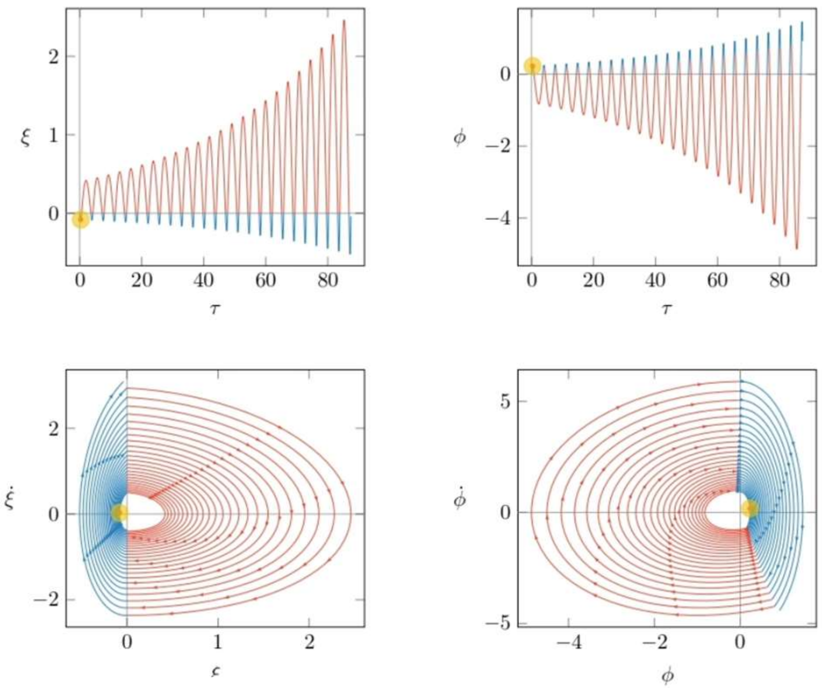

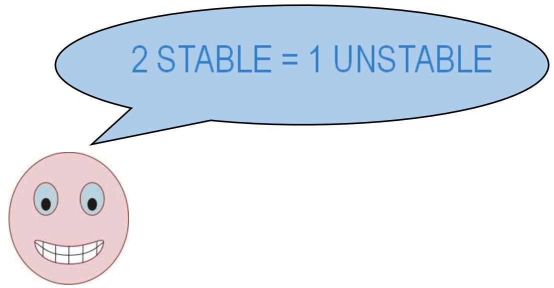

What is the lesson for continua? Hill comparison solid in plasticity

$$\dot{\boldsymbol{\sigma}} = \mathcal{C}\dot{\boldsymbol{\varepsilon}}, \quad \mathcal{C} = \mathcal{E} - \frac{1}{H + \boldsymbol{Q} \cdot \mathcal{E}\boldsymbol{P}} \mathcal{E}\boldsymbol{P} \otimes \mathcal{E}\boldsymbol{Q}$$

Hill

$$\dot{\boldsymbol{\sigma}} = \mathcal{E}\dot{\boldsymbol{\varepsilon}}$$

Elastic

A piecewise incrementally linear (thus nonlinear) problem is simplified to 2 linear problems

THIS APPROXIMATION MAY NOT BE INCLUSIVE OF IMPORTANT INSTABILITY PHENOMENA!

How to link structures to solids?

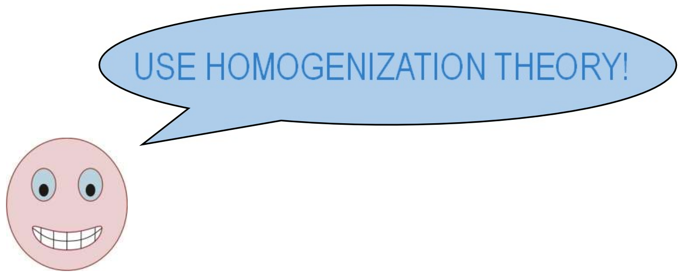

Note: our structures are not intelligent at all, as they have to blindly follow our equations

Idea: artificial materials

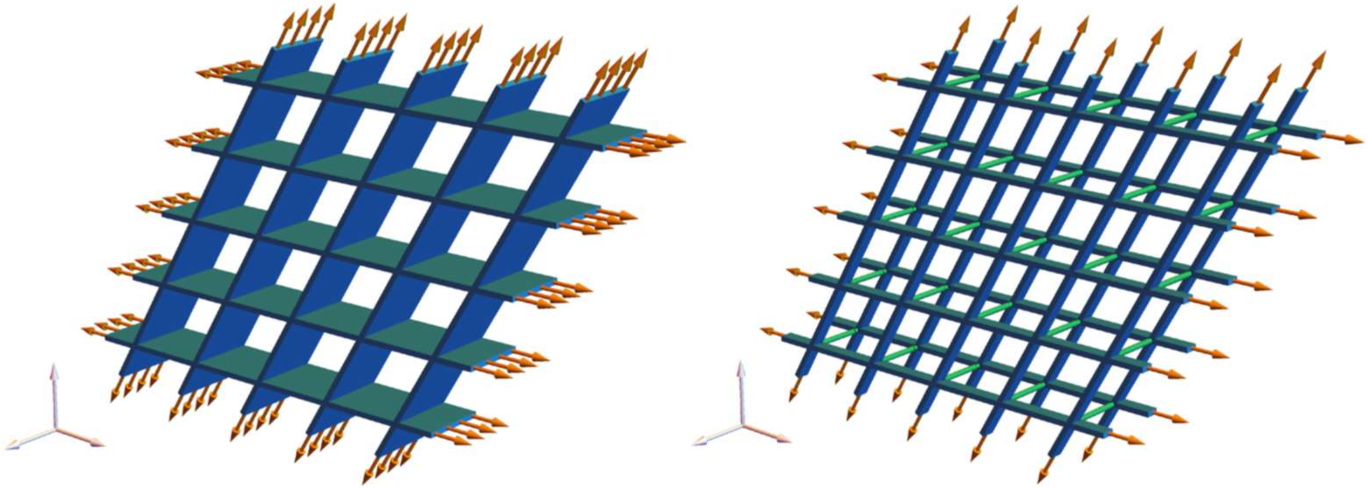

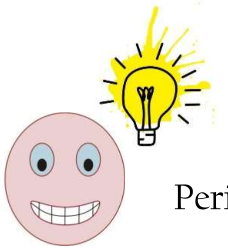

Periodic 2D grid of axially and flexurally deformable elastic rods, axially preloaded and subject to in-plane incremental deformation

Time-harmonic dynamics of prestressed rods

$$-\gamma(\lambda_0)\,\omega^2 u(s) - A(\lambda_0)\,u''(s) = 0$$

Mass density

Axial stiffness

Bending stiffness

Pre-load

Rotational inertia

$$-\gamma(\lambda_0)\,\omega^2 v(s) + \gamma_r(\lambda_0)\,\omega^2 v''(s) + B(\lambda_0)\,v''''(s) - P(\lambda_0)\,v''(s) = 0$$

$$u(s) = \sum_{j=1}^{2} C_j^u\, e^{i\,\beta_j^u\, s}\,, \qquad v(s) = \sum_{j=1}^{4} C_j^v\, e^{i\,\beta_j^v\, s}$$

$$\beta_{1,2}^u = \pm\frac{\tilde{\omega}}{l}\,, \qquad \beta_{1,2,3,4}^v = \pm\frac{1}{l\sqrt{2}}\sqrt{-p + r\,\tilde{\omega}^2 \pm \sqrt{p^2 + (4\Lambda^2 - 2\,p\,r)\,\tilde{\omega}^2 + r^2\,\tilde{\omega}^4}}$$

$$\boldsymbol{u}(s) = \boldsymbol{N}(s;\omega, P)\,\boldsymbol{q}$$

Matrix collecting prestress-dependent shape functions

Displacements & rotations at the ends of the rod

Energies for the prestressed rod

1) Kinetic energy

$$\mathcal{T}_k = \frac{1}{2}\int_0^{l_k} \gamma_k \left(\dot{u}_k(s_k,t)^2 + \dot{v}_k(s_k,t)^2\right) ds_k + \frac{1}{2}\int_0^{l_k} \gamma_{r,k}\dot{v}_k'(s_k,t)^2 ds_k$$

2) Elastic energy

$$\mathcal{E}_k = \frac{1}{2}\int_0^{l_k} \left(A_k\, u_k'(s_k,t)^2 + B_k\, v_k''(s_k,t)^2\right) ds_k$$

3) Potential energy

$$\mathcal{V}_k^g = \frac{1}{2}P_k \int_0^{l_k} v_k'(s_k,t)^2\, ds_k$$

Prestress dependent stiffness matrix

$$
\boldsymbol{K}_k = \begin{bmatrix}
\frac{A_k}{l_k} & 0 & 0 & -\frac{A_k}{l_k} & 0 & 0 \\
0 & \frac{12B_k}{l_k^3}\varphi_1(p_k) & \frac{6B_k}{l_k^2}\varphi_2(p_k) & 0 & -\frac{12B_k}{l_k^3}\varphi_1(p_k) & \frac{6B_k}{l_k^2}\varphi_2(p_k) \\
0 & \frac{6B_k}{l_k^2}\varphi_2(p_k) & \frac{4B_k}{l_k}\varphi_3(p_k) & 0 & -\frac{6B_k}{l_k^2}\varphi_2(p_k) & \frac{2B_k}{l_k}\varphi_4(p_k) \\
-\frac{A_k}{l_k} & 0 & 0 & \frac{A_k}{l_k} & 0 & 0 \\
0 & -\frac{12B_k}{l_k^3}\varphi_1(p_k) & -\frac{6B_k}{l_k^2}\varphi_2(p_k) & 0 & \frac{12B_k}{l_k^3}\varphi_1(p_k) & -\frac{6B_k}{l_k^2}\varphi_2(p_k) \\
0 & \frac{6B_k}{l_k^2}\varphi_2(p_k) & \frac{2B_k}{l_k}\varphi_4(p_k) & 0 & -\frac{6B_k}{l_k^2}\varphi_2(p_k) & \frac{4B_k}{l_k}\varphi_3(p_k)
\end{bmatrix}
$$

prestress $p_k = P_k l_k^2 / B_k$

$$
\varphi_1(p_k) = \frac{p_k^{3/2}}{12\left(\sqrt{p_k} - 2\tanh\left(\sqrt{p_k}/2\right)\right)}, \qquad \varphi_2(p_k) = \frac{p_k}{6\sqrt{p_k}\coth\left(\sqrt{p_k}/2\right) - 12},
$$

$$
\varphi_3(p_k) = \frac{p_k\cosh\left(\sqrt{p_k}\right) - \sqrt{p_k}\sinh\left(\sqrt{p_k}\right)}{4\sqrt{p_k}\sinh\left(\sqrt{p_k}\right) - 8\cosh\left(\sqrt{p_k}\right) + 8}, \qquad \varphi_4(p_k) = \frac{\sqrt{p_k}\left(\sinh\left(\sqrt{p_k}\right) - \sqrt{p_k}\right)}{\left(4\sqrt{p_k}\coth\left(\sqrt{p_k}/2\right) - 8\right)\sinh^2\left(\sqrt{p_k}/2\right)}
$$

The governing equations

- Compatibility of displacements and rotations at the central node of the unit cell

$$
\begin{aligned}
&v_1(1)=v_3(0), &&v_2(1)=v_4(0), &&v_1(1)=-u_2(1),\\
&u_1(1)=u_3(0), &&u_2(1)=u_4(0), &&v_2(1)=u_1(1),\\
&v_1'(1)=\alpha\, v_2'(1), &&\alpha\, v_2'(1)=v_3'(0), &&v_3'(0)=\alpha\, v_4'(0),
\end{aligned}
$$

- equilibrium of the central node

$$
u_3'(0)-u_1'(1)-\frac{4\,\alpha}{\chi\lambda_2^2}\,v_4'''(0)-\frac{4}{\chi\alpha\lambda_2^2}\,\tilde{\omega}_1^2\,v_4'(0)+\frac{4\,\alpha}{\chi\lambda_2^2}\,v_2'''(1)+\frac{4}{\chi\alpha\lambda_2^2}\tilde{\omega}_1^2\,v_2'(1)=0,
$$

- Floquet-Bloch boundary conditions

$$
\begin{aligned}
u_3(1)&=u_1(0)\,e^{i\,K_1},\\
v_3(1)&=v_1(0)\,e^{i\,K_1},\\
v_3'(1)&=v_1'(0)\,e^{i\,K_1},\\
u_3'(1)&=u_1'(0)\,e^{i\,K_1},\\
v_3'''(1)+\tilde{\omega}_1^2\,v_3'(1)&=(v_1'''(0)+\tilde{\omega}_1^2\,v_1'(0))\,e^{i\,K_1},\\
v_3''(1)&=v_1''(0)\,e^{i\,K_1},\\
u_4(1)&=u_2(0)\,e^{i\,K_2/\alpha},\\
v_4(1)&=v_2(0)\,e^{i\,K_2/\alpha},\\
v_4'(1)&=v_2'(0)\,e^{i\,K_2/\alpha}\\
u_4'(1)&=u_2'(0)\,e^{i\,K_2/\alpha},\\
v_4'''(1)+\frac{\tilde{\omega}_1^2}{\alpha^2}\,v_4'(1)&=\left(v_2'''(0)+\frac{\tilde{\omega}_1^2}{\alpha^2}\,v_2'(0)\right)\,e^{i\,K_2/\alpha},\\
v_4''(1)&=v_2''(0)\,e^{i\,K_2/\alpha},
\end{aligned}
$$

Bloch wave vector comps.

Dispersion equation

$$\alpha = l_1/l_2 \quad \chi = A_1/A_2$$

$$\boxed{\boldsymbol{A}(\tilde{\omega}_1, \boldsymbol{K}, \lambda_1, \lambda_2, \alpha, \chi)\,\boldsymbol{c} = \boldsymbol{0}}$$

$$\lambda_1 = 2\,l_1\sqrt{A_1/I_1} \quad \lambda_2 = 2\,l_2\sqrt{A_2/I_2}$$

Wave vector

$$\Omega = \frac{4l_1^2\omega}{\pi^2\sqrt{EI_1/(\rho A_1)}}$$

Dispersion equation

$$\boxed{\det \boldsymbol{A}(\Omega, \boldsymbol{K}, \lambda_1, \lambda_2, \alpha, \chi) = 0}$$

Dispersion surfaces

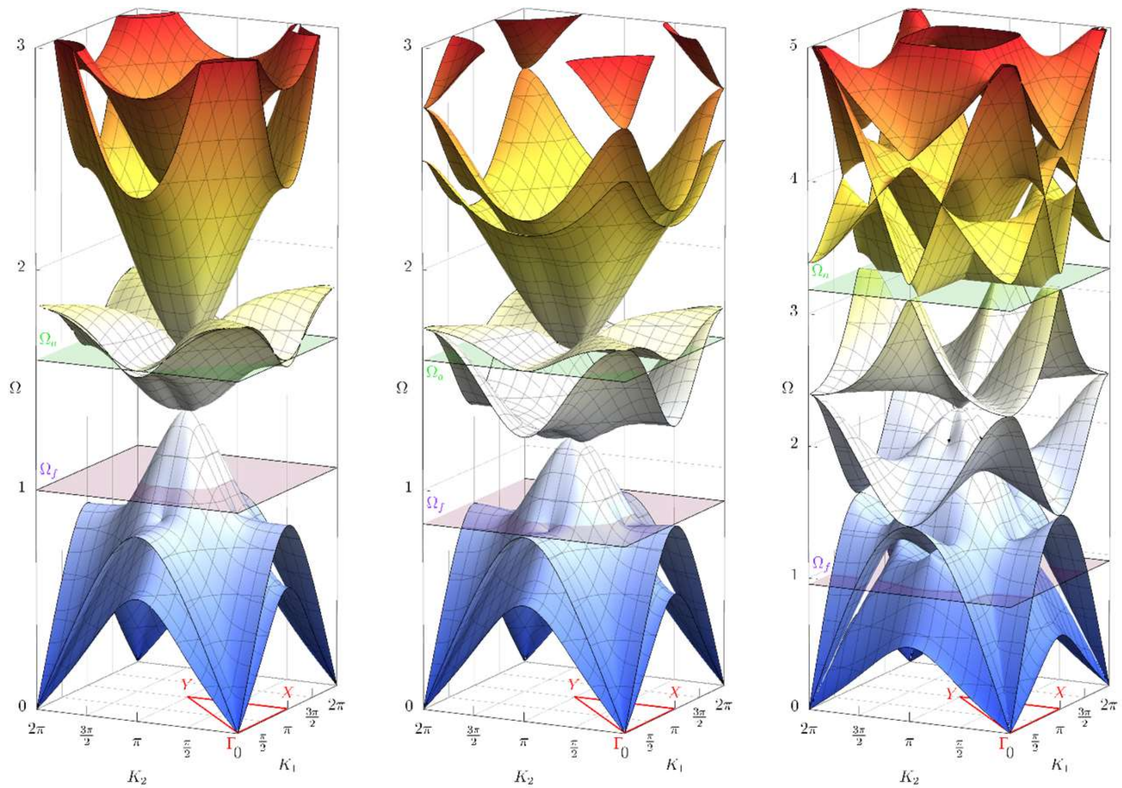

Euler-Bernulli Rayleigh (slender)

effects of rotational inertia become evident at high frequency

Completely flat band and Dirac cone

Flat band

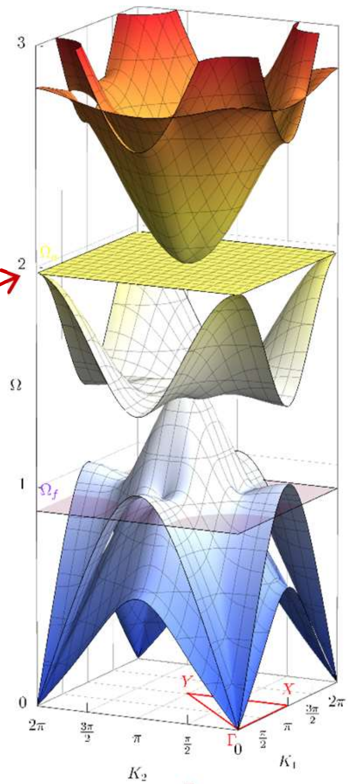

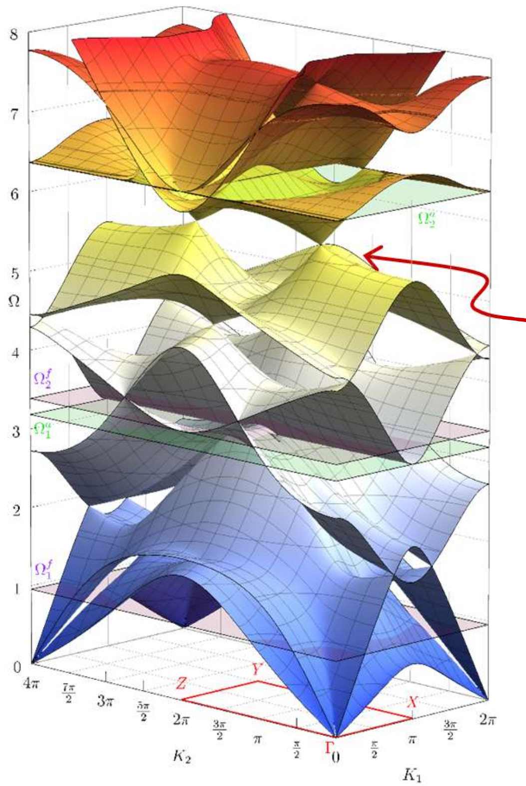

Dirac cone

Square lattice

Slenderness 6.192

Rectangular lattice ($\alpha = l_1 / l_2 = 2$)

Slenderness $\lambda_1 = 5$, $\lambda_2 = 10$

(infinite set of standing waves propagating at $\Omega = 1.971$)

Homogenization of a lattice of elastic rods

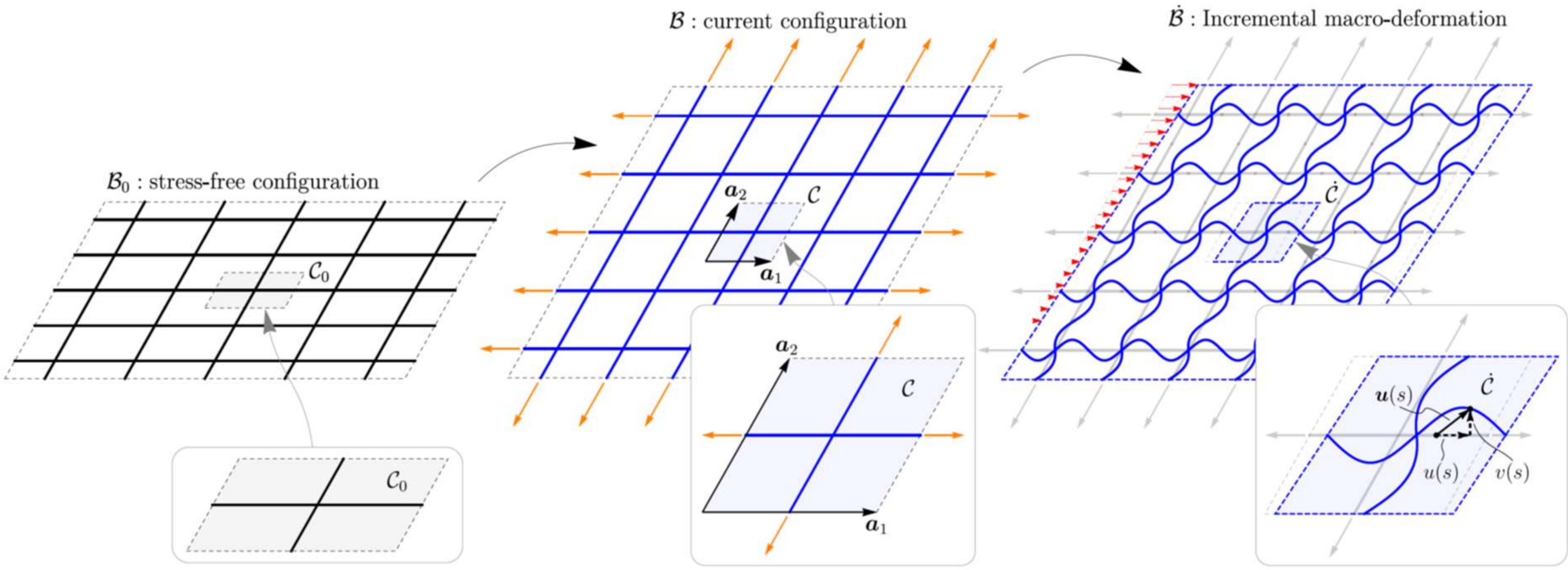

Periodic 2D lattice of axially and flexurally deformable elastic rods, axially preloaded
and subject to in-plane incremental deformation

The lattice is spatially periodic

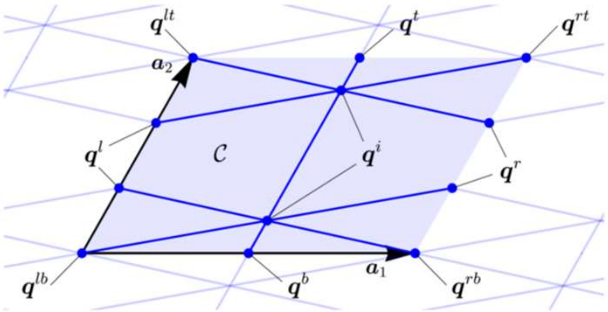

Unit cell

- In dynamics, Bloch theorem

$$\boldsymbol{u}(\boldsymbol{x} + n_j \boldsymbol{a}_j) = \boldsymbol{u}(\boldsymbol{x})\, e^{i\,\boldsymbol{k}\cdot(n_j \boldsymbol{a}_j)}$$

- In statics Cauchy-Born hypothesis

$$\boldsymbol{q}_u^{(j)} = \tilde{\boldsymbol{q}}_u^{(j)} + \boldsymbol{L}\,\boldsymbol{x}_j\,, \qquad \boldsymbol{q}_\theta^{(j)} = \tilde{\boldsymbol{q}}_\theta^{(j)}$$

The equivalent continuum

Incremental strain energy density

$$\mathcal{W}(\boldsymbol{L}) = \underbrace{\boldsymbol{T} \cdot \boldsymbol{L}}_{\mathcal{W}_1(\boldsymbol{L})} + \underbrace{\mathbb{C}[\boldsymbol{L}] \cdot \boldsymbol{L}/2}_{\mathcal{W}_2(\boldsymbol{L})}$$

$$\mathbb{C} = \mathbb{E} + \boldsymbol{I} \boxtimes \boldsymbol{T}$$

$$\dot{\boldsymbol{S}} = \mathbb{C}[\boldsymbol{L}]$$

In statics: 1° and 2° order matching of strain energy

First-order matching

$$\underbrace{\boldsymbol{T} \cdot \boldsymbol{L}}_{\text{Continuum}} = \underbrace{\frac{1}{|\mathcal{C}|} \boldsymbol{f}_{\boldsymbol{P}} \cdot \boldsymbol{q}(\tilde{\boldsymbol{q}}^*(\boldsymbol{L}), \boldsymbol{L})}_{\text{Lattice}}$$

Second-order matching

$$\underbrace{\frac{1}{2} \mathbb{C}[\boldsymbol{L}] \cdot \boldsymbol{L}}_{\text{Continuum}} = \underbrace{\frac{1}{|\mathcal{C}|} \mathcal{E}(\boldsymbol{L})}_{\text{Lattice}}$$

In dynamics: match on asymptotics

Solution of a sequence of linear systems

$$
\begin{aligned}
\mathcal{O}(\epsilon^0): &\quad \boldsymbol{A}_{\boldsymbol{n}}^{*(0)}\, \boldsymbol{q}_{\boldsymbol{n}}^{*(0)} = \boldsymbol{0}\,,\\
\mathcal{O}(\epsilon^1): &\quad \boldsymbol{A}_{\boldsymbol{n}}^{*(0)}\, \boldsymbol{q}_{\boldsymbol{n}}^{*(1)} + \boldsymbol{A}_{\boldsymbol{n}}^{*(1)}\, \boldsymbol{q}_{\boldsymbol{n}}^{*(0)} = \boldsymbol{0}\,,\\
\mathcal{O}(\epsilon^2): &\quad \boldsymbol{A}_{\boldsymbol{n}}^{*(0)}\, \boldsymbol{q}_{\boldsymbol{n}}^{*(2)} + \boldsymbol{A}_{\boldsymbol{n}}^{*(1)}\, \boldsymbol{q}_{\boldsymbol{n}}^{*(1)} + \boldsymbol{A}_{\boldsymbol{n}}^{*(2)}\, \boldsymbol{q}_{\boldsymbol{n}}^{*(0)} = \boldsymbol{0}\,,\\
\vdots &\qquad\qquad\qquad\qquad \vdots\\
\mathcal{O}(\epsilon^j): &\quad \boldsymbol{A}_{\boldsymbol{n}}^{*(0)}\, \boldsymbol{q}_{\boldsymbol{n}}^{*(j)} + \sum_{h=1}^{j} \boldsymbol{A}_{\boldsymbol{n}}^{*(h)}\, \boldsymbol{q}_{\boldsymbol{n}}^{*(j-h)} = \boldsymbol{0}, \qquad \forall j > 0
\end{aligned}
$$

A framework already available in the literature, see N. Triantafyllidis, P. Ponte Castañeda, J.R. Willis

Lattice homogenization & material instabilities

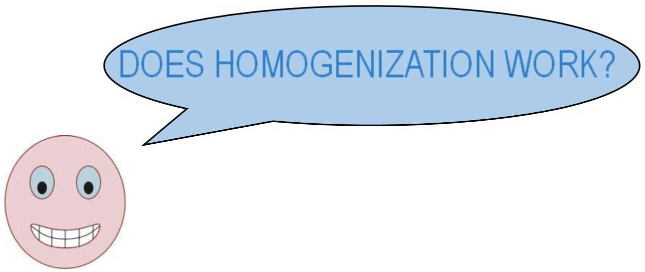

Not always when instabilities are concerned!

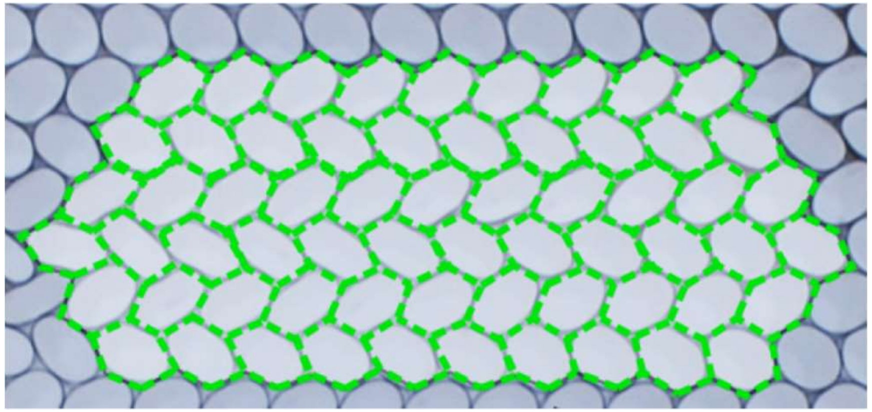

Microscopic bifurcation

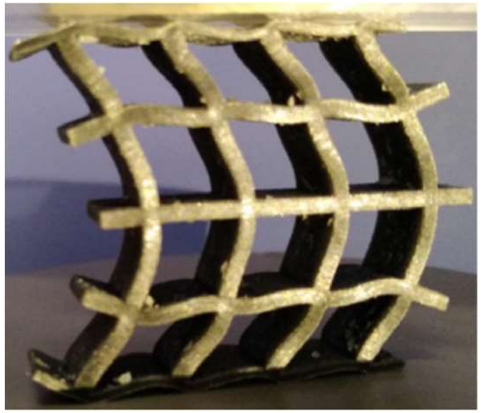

Macroscopic bifurcation

- Only macroscopic bifurcations are captured by homogenization
- Macroscopic bifurcations coincide with loss of ellipticity in the equivalent solid
- Macroscopic bifurcations are localized into shear o dilatational bands
- Microscopic bifurcation is a microstructural response

These results are due to N. Triantafyllidis, P. Ponte Castañeda, and J.R. Willis

Homogenization of a prestressed lattice: Results

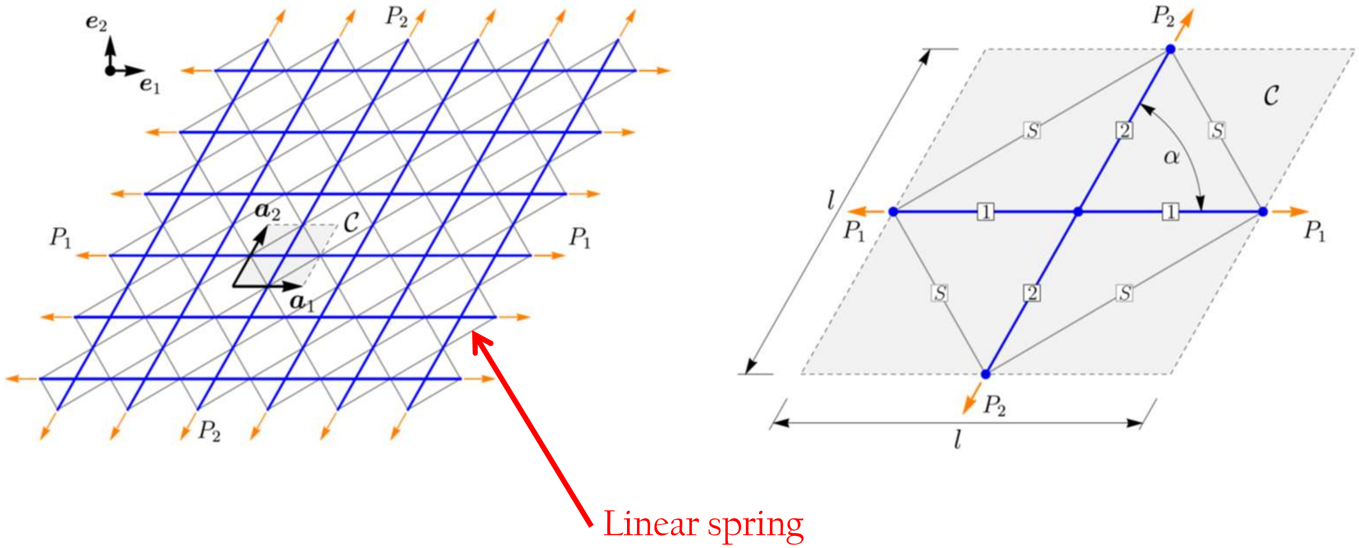

Results 1: Prestress tensor in the equivalent solid

Determined at first-order:

$$\boldsymbol{T} = \left(\frac{P_1}{l \sin \alpha} + \frac{P_2 \cos^2 \alpha}{l \sin \alpha} \right) \boldsymbol{e}_1 \otimes \boldsymbol{e}_1 + \frac{P_2 \cos \alpha}{l} (\boldsymbol{e}_1 \otimes \boldsymbol{e}_2 + \boldsymbol{e}_2 \otimes \boldsymbol{e}_1) + \frac{P_2 \sin \alpha}{l} \boldsymbol{e}_2 \otimes \boldsymbol{e}_2$$

Results at second-order: 10 components!

$$
\begin{aligned}
\bar{\mathbb{C}}^{G}_{1111} = \frac{1}{2d\sin\alpha} \Big(& \sinh\left(\frac{\sqrt{p_2}}{2}\right) \Big(\sqrt{p_1} p_2 \phi \cosh\left(\frac{\sqrt{p_1}}{2}\right) (\cos(4\alpha)(\Lambda_1^2 - p_2\phi) + 4\Lambda_1^2 \cos(2\alpha) + 11\Lambda_1^2 + p_2\phi) \\
& - 2\sinh\left(\frac{\sqrt{p_1}}{2}\right) (\cos(4\alpha)(\Lambda_1^2(p_1+p_2\phi) - p_2^2\phi^2) + \Lambda_1^2(p_1+p_2\phi)(4\cos(2\alpha)+11) + p_2^2\phi^2) \Big) \\
& + p_1\sqrt{p_2}\sinh\left(\frac{\sqrt{p_1}}{2}\right)\cosh\left(\frac{\sqrt{p_2}}{2}\right)(\cos(4\alpha)(\Lambda_1^2 - p_2\phi) + 4\Lambda_1^2\cos(2\alpha) + 11\Lambda_1^2 + p_2\phi) \Big)
\end{aligned}
$$

$$
\begin{aligned}
\bar{\mathbb{C}}^{G}_{1122} = \frac{4\sin\alpha\cos^2\alpha}{d} \Big(& \sinh\left(\frac{\sqrt{p_2}}{2}\right) \Big(\sqrt{p_1} p_2\phi\cosh\left(\frac{\sqrt{p_1}}{2}\right)(\Lambda_1^2 - p_2\phi) - 2\sinh\left(\frac{\sqrt{p_1}}{2}\right)(\Lambda_1^2(p_1+p_2\phi) - p_2^2\phi^2) \Big) \\
& + p_1\sqrt{p_2}\sinh\left(\frac{\sqrt{p_1}}{2}\right)\cosh\left(\frac{\sqrt{p_2}}{2}\right)(\Lambda_1^2 - p_2\phi) \Big)
\end{aligned}
$$

$$
\begin{aligned}
\bar{\mathbb{C}}^{G}_{1112} = \frac{-2\cos\alpha}{d} \Big(& \sinh\left(\frac{\sqrt{p_2}}{2}\right) \Big(2\sinh\left(\frac{\sqrt{p_1}}{2}\right)(\cos(2\alpha)(\Lambda_1^2(p_1+p_2\phi) - p_2^2\phi^2) + \Lambda_1^2(p_1+p_2\phi) + p_2^2\phi^2) \\
& - \sqrt{p_1}p_2\phi\cosh\left(\frac{\sqrt{p_1}}{2}\right)(\cos(2\alpha)(\Lambda_1^2 - p_2\phi) + \Lambda_1^2 + p_2\phi) \Big) \\
& + p_1\sqrt{p_2}\sinh\left(\frac{\sqrt{p_1}}{2}\right)\cosh\left(\frac{\sqrt{p_2}}{2}\right)(\cos(2\alpha)(p_2\phi - \Lambda_1^2) - \Lambda_1^2 - p_2\phi) \Big)
\end{aligned}
$$

$$
\begin{aligned}
\bar{\mathbb{C}}^{G}_{1121} = \frac{4\cos\alpha}{d} \Big(& \sinh\left(\frac{\sqrt{p_2}}{2}\right) \Big(2\sinh\left(\frac{\sqrt{p_1}}{2}\right)(p_1p_2\phi - \cos^2\alpha(\Lambda_1^2(p_1+p_2\phi) - p_2^2\phi^2)) + \sqrt{p_1}p_2\phi\cos^2\alpha\cosh\left(\frac{\sqrt{p_1}}{2}\right)(\Lambda_1^2 - p_2\phi) \Big) \\
& + p_1\sqrt{p_2}\cos^2\alpha\sinh\left(\frac{\sqrt{p_1}}{2}\right)\cosh\left(\frac{\sqrt{p_2}}{2}\right)(\Lambda_1^2 - p_2\phi) \Big)
\end{aligned}
$$

$$
\begin{aligned}
\bar{\mathbb{C}}^{G}_{2222} = \frac{2\sin\alpha}{d} \Big(& \sinh\left(\frac{\sqrt{p_2}}{2}\right) \Big(\sqrt{p_1}p_2\phi\cosh\left(\frac{\sqrt{p_1}}{2}\right)(\cos(2\alpha)(p_2\phi - \Lambda_1^2) + \Lambda_1^2 + p_2\phi) \\
& - 2\sinh\left(\frac{\sqrt{p_1}}{2}\right)(-\cos(2\alpha)(\Lambda_1^2(p_1+p_2\phi) - p_2^2\phi^2) + \Lambda_1^2(p_1+p_2\phi) + p_2^2\phi^2) \Big) \\
& + p_1\sqrt{p_2}\sinh\left(\frac{\sqrt{p_1}}{2}\right)\cosh\left(\frac{\sqrt{p_2}}{2}\right)(\cos(2\alpha)(p_2\phi - \Lambda_1^2) + \Lambda_1^2 + p_2\phi) \Big)
\end{aligned}
$$

$$
\begin{aligned}
\bar{\mathbb{C}}^{G}_{2212} = \frac{4\sin^2\alpha\cos\alpha}{d} \Big(& \sinh\left(\frac{\sqrt{p_2}}{2}\right) \Big(\sqrt{p_1}p_2\phi\cosh\left(\frac{\sqrt{p_1}}{2}\right)(\Lambda_1^2 - p_2\phi) - 2\sinh\left(\frac{\sqrt{p_1}}{2}\right)(\Lambda_1^2(p_1+p_2\phi) - p_2^2\phi^2) \Big) \\
& + p_1\sqrt{p_2}\sinh\left(\frac{\sqrt{p_1}}{2}\right)\cosh\left(\frac{\sqrt{p_2}}{2}\right)(\Lambda_1^2 - p_2\phi) \Big)
\end{aligned}
$$

$$
\begin{aligned}
\bar{\mathbb{C}}^{G}_{2221} = \frac{2\cos\alpha}{d} \Big(& \sinh\left(\frac{\sqrt{p_2}}{2}\right) \Big(\sqrt{p_1}p_2\phi\cosh\left(\frac{\sqrt{p_1}}{2}\right)(\cos(2\alpha)(p_2\phi - \Lambda_1^2) + \Lambda_1^2 + p_2\phi) \\
& - 2\sinh\left(\frac{\sqrt{p_1}}{2}\right)(-\cos(2\alpha)(\Lambda_1^2(p_1+p_2\phi) - p_2^2\phi^2) + \Lambda_1^2(p_1+p_2\phi) + p_2\phi(2p_1+p_2\phi)) \Big) \\
& + p_1\sqrt{p_2}\sinh\left(\frac{\sqrt{p_1}}{2}\right)\cosh\left(\frac{\sqrt{p_2}}{2}\right)(\cos(2\alpha)(p_2\phi - \Lambda_1^2) + \Lambda_1^2 + p_2\phi) \Big)
\end{aligned}
$$

$$
\begin{aligned}
\bar{\mathbb{C}}^{G}_{1212} = \frac{-2\sin\alpha}{d} \Big(& \sinh\left(\frac{\sqrt{p_2}}{2}\right) \Big(2\sinh\left(\frac{\sqrt{p_1}}{2}\right)(\cos(2\alpha)(\Lambda_1^2(p_1+p_2\phi) - p_2^2\phi^2) + \Lambda_1^2(p_1+p_2\phi) + p_2^2\phi^2) \\
& - \sqrt{p_1}p_2\phi\cosh\left(\frac{\sqrt{p_1}}{2}\right)(\cos(2\alpha)(\Lambda_1^2 - p_2\phi) + \Lambda_1^2 + p_2\phi) \Big) \\
& + p_1\sqrt{p_2}\sinh\left(\frac{\sqrt{p_1}}{2}\right)\cosh\left(\frac{\sqrt{p_2}}{2}\right)(\cos(2\alpha)(p_2\phi - \Lambda_1^2) - \Lambda_1^2 - p_2\phi) \Big)
\end{aligned}
$$

$$
\begin{aligned}
\bar{\mathbb{C}}^{G}_{1221} = \frac{-4\sin\alpha}{d} \Big(& \sinh\left(\frac{\sqrt{p_2}}{2}\right) \Big(2\sinh\left(\frac{\sqrt{p_1}}{2}\right)(\cos^2\alpha(\Lambda_1^2(p_1+p_2\phi) - p_2^2\phi^2) - p_1p_2\phi) \\
& + \sqrt{p_1}p_2\phi\cos^2\alpha\cosh\left(\frac{\sqrt{p_1}}{2}\right)(p_2\phi - \Lambda_1^2) \Big) + p_1\sqrt{p_2}\cos^2\alpha\sinh\left(\frac{\sqrt{p_1}}{2}\right)\cosh\left(\frac{\sqrt{p_2}}{2}\right)(p_2\phi - \Lambda_1^2) \Big)
\end{aligned}
$$

$$
\begin{aligned}
\bar{\mathbb{C}}^{G}_{2121} = & \frac{p_1\sqrt{p_2}}{d}\sinh\left(\frac{\sqrt{p_1}}{2}\right)\cosh\left(\frac{\sqrt{p_2}}{2}\right)(\sin\alpha(\Lambda_1^2 - 5p_2\phi) + \sin(3\alpha)(\Lambda_1^2 - p_2\phi) + 4\csc(\alpha)(p_1+p_2\phi)) \\
& - 2\sin\alpha\sinh\left(\frac{\sqrt{p_2}}{2}\right)\Big(2\sinh\left(\frac{\sqrt{p_1}}{2}\right)\Big(\cos(2\alpha)(\Lambda_1^2(p_1+p_2\phi) - p_2^2\phi^2) + 2\csc^2(\alpha)(p_1+p_2\phi)^2 + \Lambda_1^2(p_1+p_2\phi) \\
& - p_2\phi(4p_1+3p_2\phi)\Big) - \sqrt{p_1}p_2\phi\cosh\left(\frac{\sqrt{p_1}}{2}\right)(\cos(2\alpha)(\Lambda_1^2 - p_2\phi) + 2\csc^2(\alpha)(p_1+p_2\phi) + (\Lambda_1^2 - 3p_2\phi))\Big)
\end{aligned}
$$

$$
\mathbb{C} = \frac{A}{l}\,\bar{\mathbb{C}}(\underbrace{p_1,\, p_2}_{\text{prestress}},\, \underbrace{\Lambda_1,\, \phi,\, \kappa,\, \alpha}_{\text{microstructure}})
$$

$$\phi = B_2/B_1$$

$$\kappa = k_S l/A$$

$$\Lambda_1 = l\sqrt{A/B_1}$$

Uniqueness/stability domains

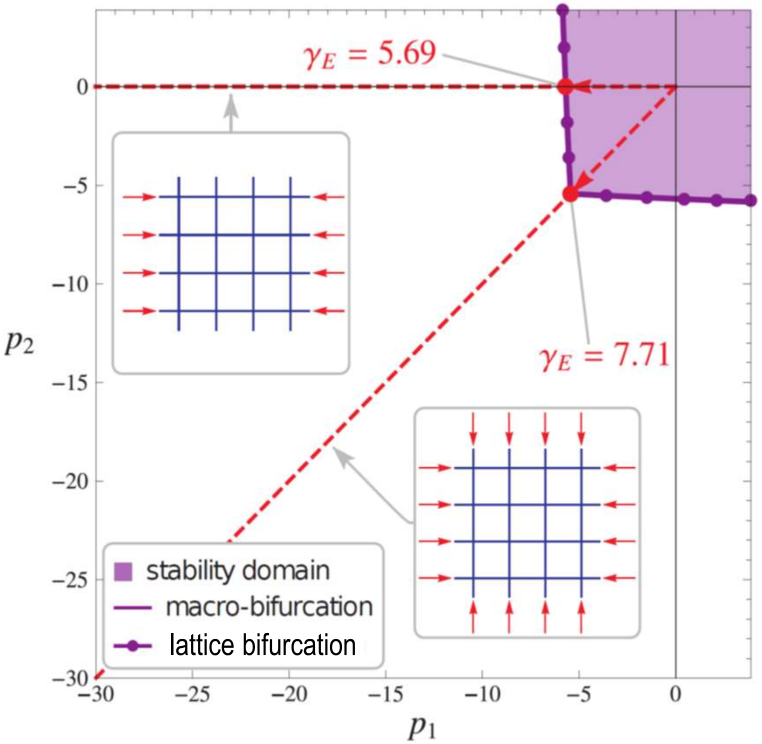

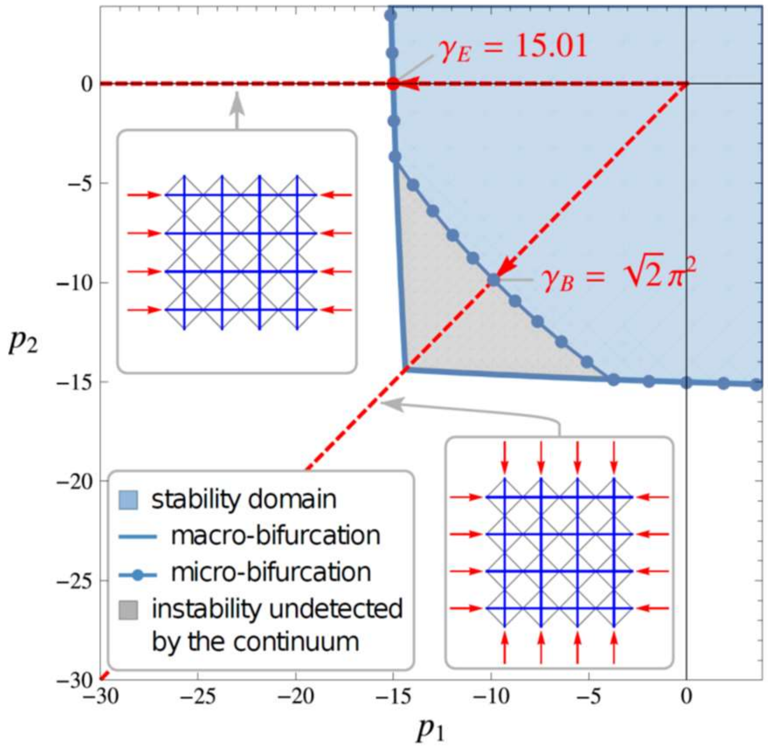

Perturbative approach to shear bands

$$\boldsymbol{G}(\boldsymbol{x}) = -\frac{1}{4\pi^2}\sum_{N=1}^{2}\int_0^{\pi} [2\cos(rk_N|\cos\alpha|)\mathrm{Ci}(rk_N|\cos\alpha|)$$

$$+2\sin(rk_N|\cos\alpha|)\mathrm{Si}(rk_N|\cos\alpha|) - i\pi\cos(rk_N|\cos\alpha|)]\frac{\boldsymbol{v}_N \otimes \boldsymbol{w}_N}{\rho\, c_N^2}d\alpha$$

$$k_N = \omega / c_N \longleftarrow$$

eigenvalues right and left eigenvectors
of the acoustic tensor

Green's function for incremental deformation of a prestressed body

Bigoni & Capuani	JMPS 2002
Bigoni & Capuani	JMPS 2005
Piccolroaz, Bigoni & Willis	JMPS 2006

Perturbative approach to shear bands

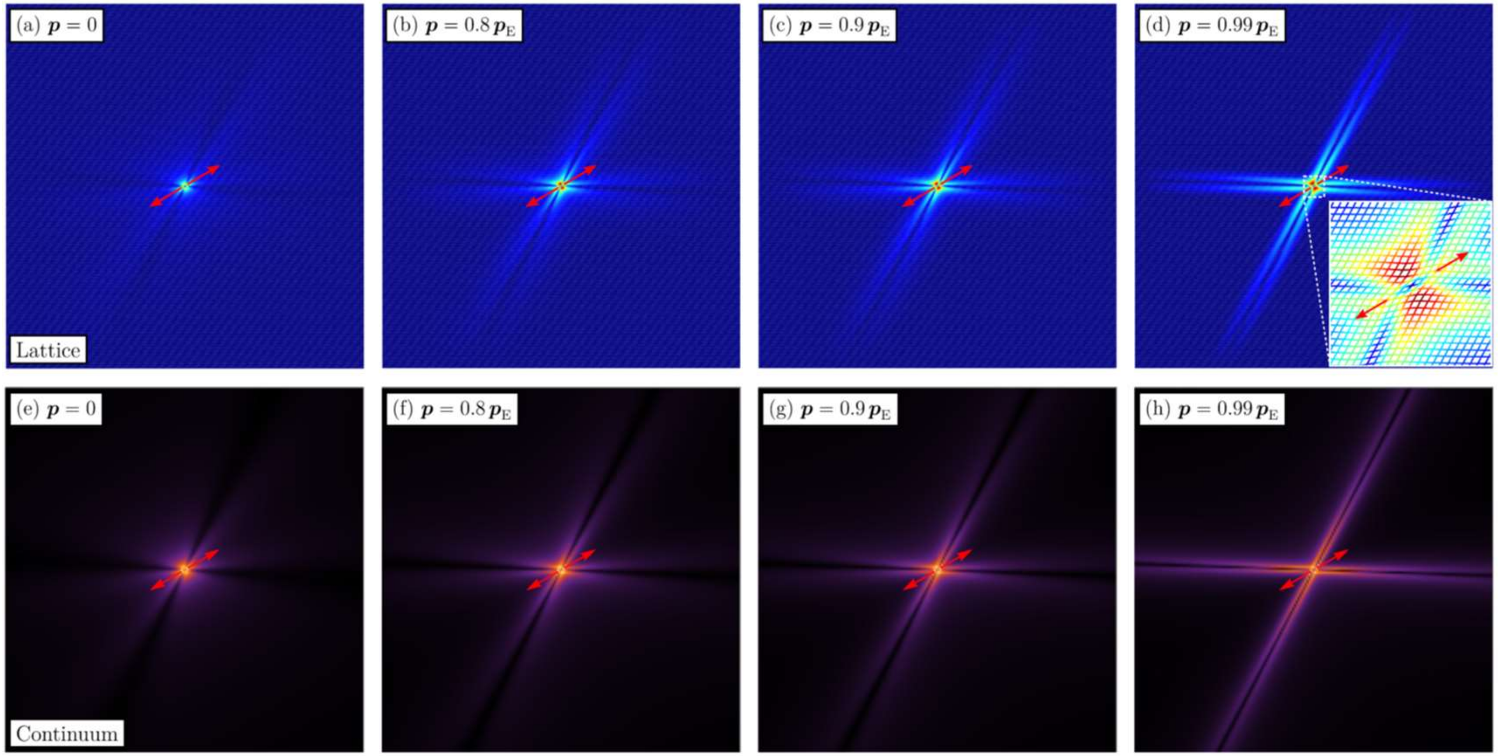

Perturbative approach to shear bands

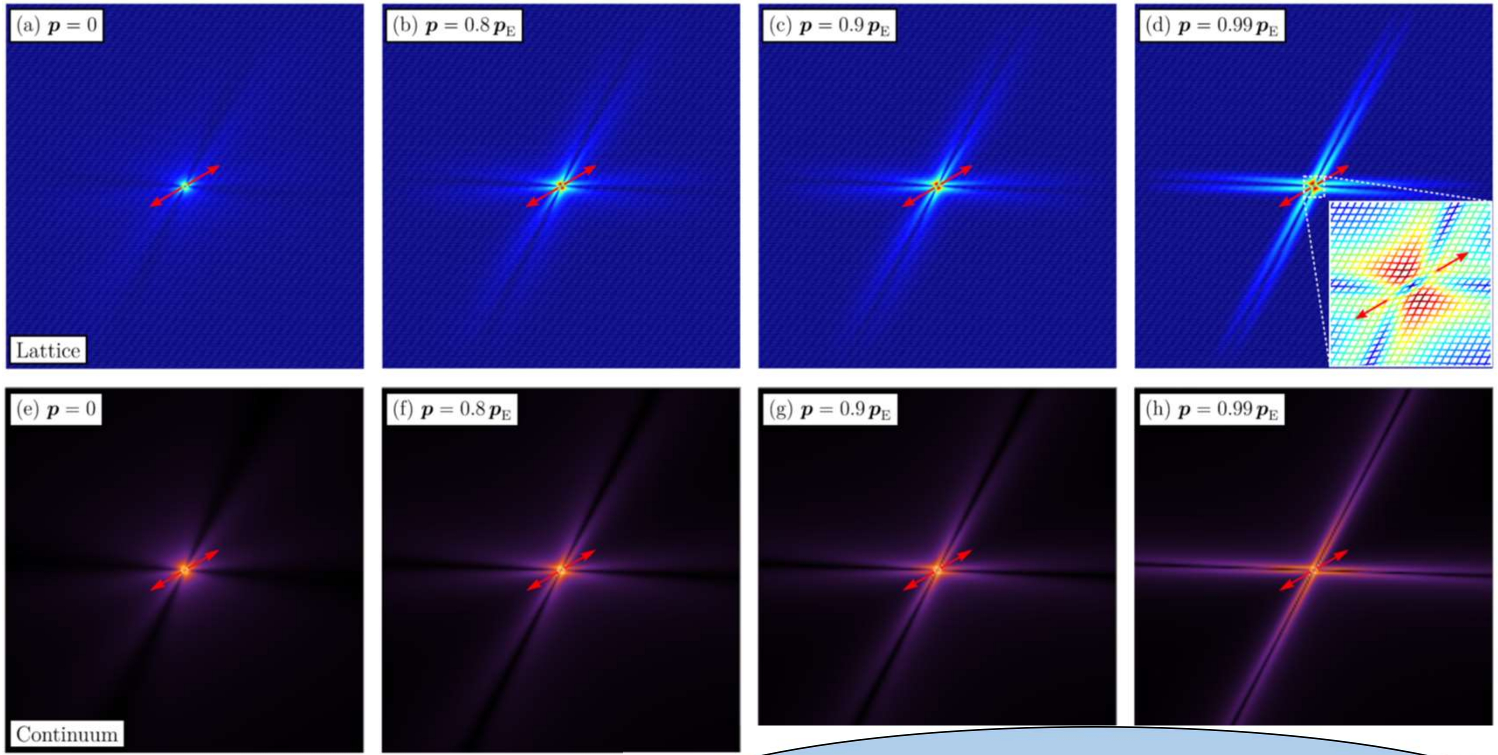

THE ARCHITECTED MATERIAL SHOWS SHEAR BANDS OCCURRING WITHIN THE ELASTIC RANGE! THE SHEAR BANDS CAN BE ACTIVATED OR INHIBITED WITH THE PRESTRESS

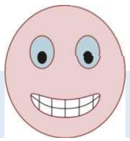

Is the stability domain always unbounded?

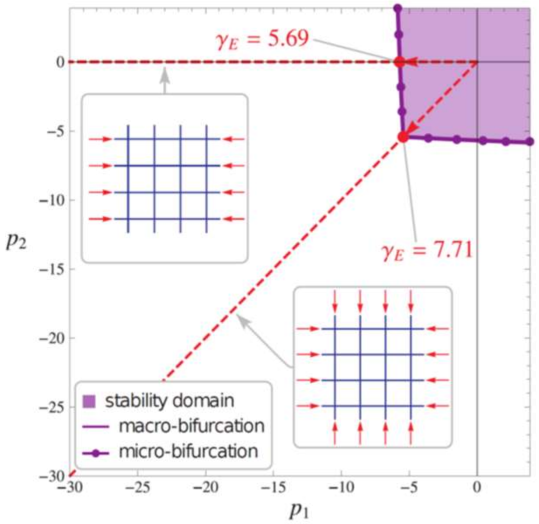

Open in tension

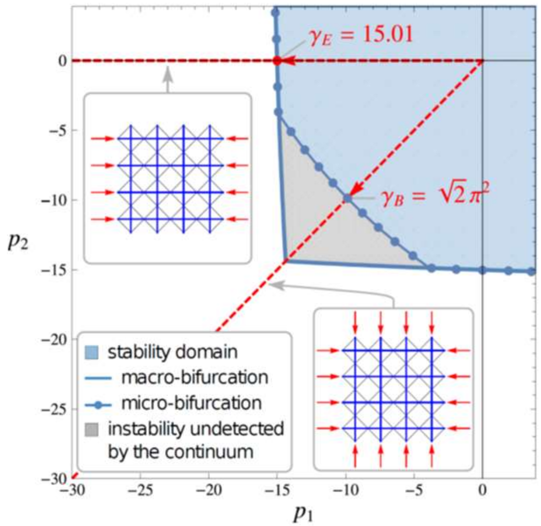

Open in tension

These two domains are open because structures do not buckle in tension

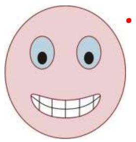

... but structures MAY buckle in tension!

Enhancing elastic rods with sliders

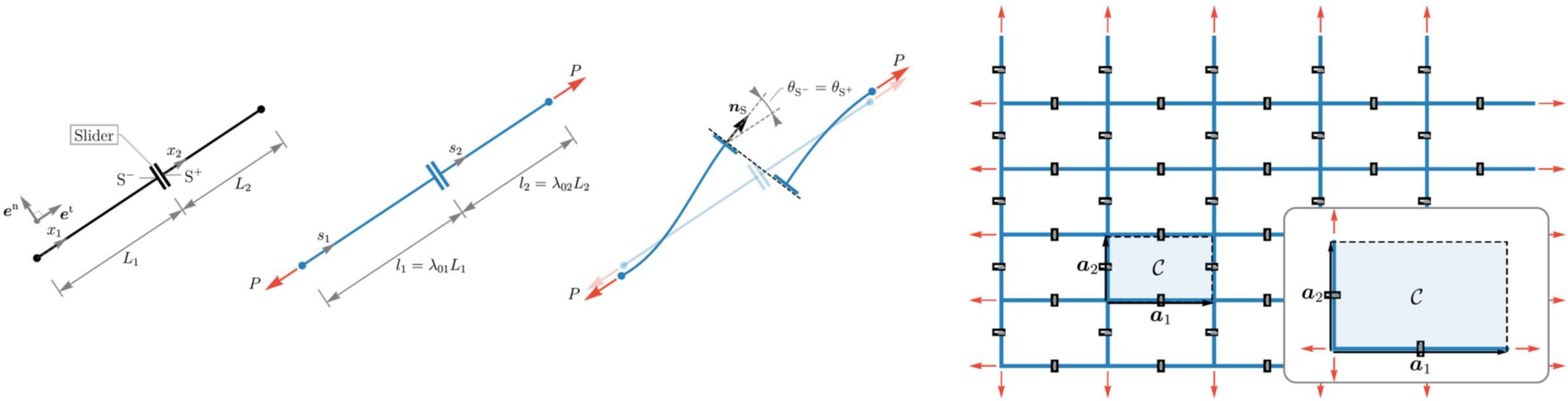

Now buckling in tension occurs!

Bounded stability domain

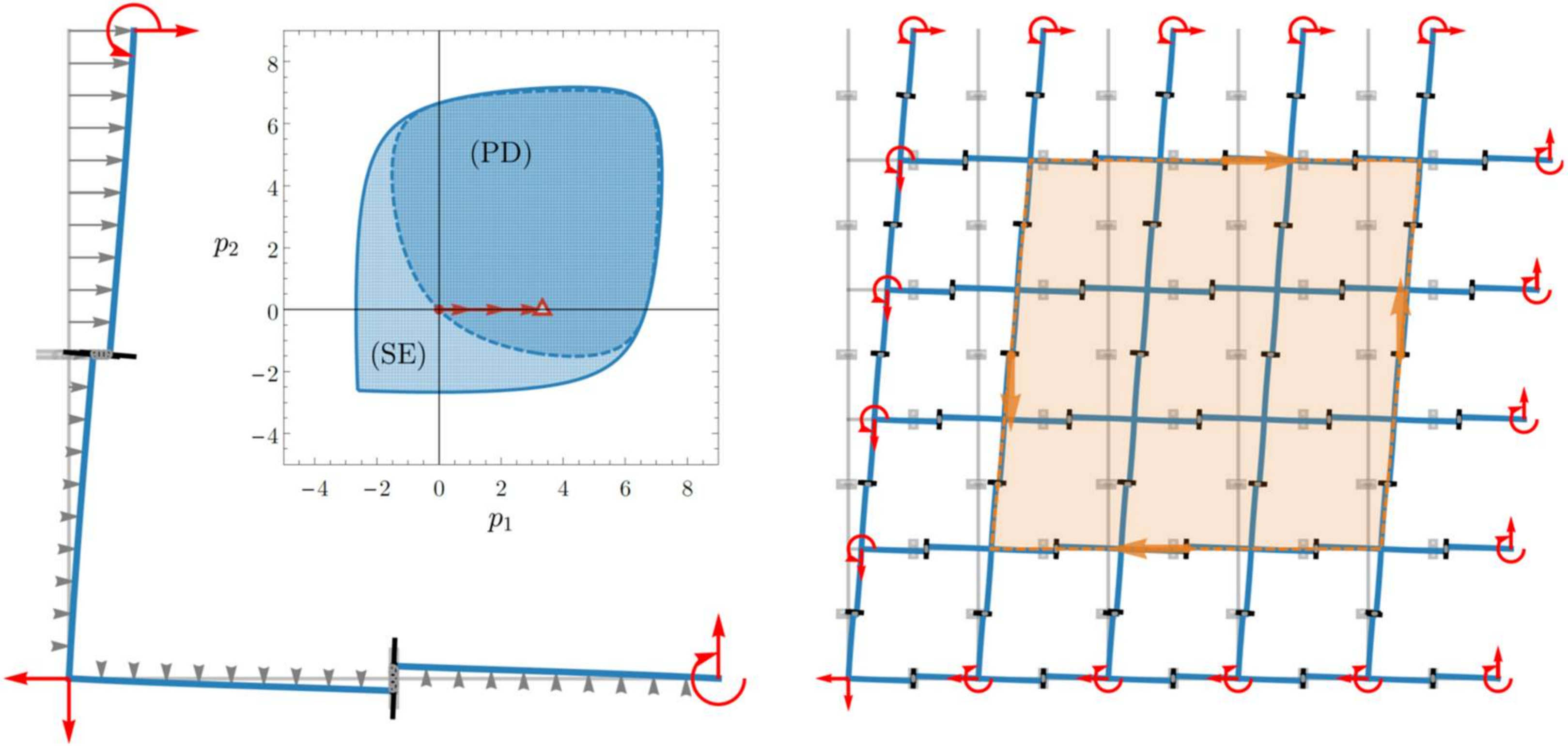

Bordiga, G., Piccolroaz, A., Bigoni, D. (2023) Tensile material instabilities in elastic beam lattices lead to a closed stability domain. *Philosophical Transactions of the Royal Society A*, **380**, 20210388.

An elastic grid subject to follower forces

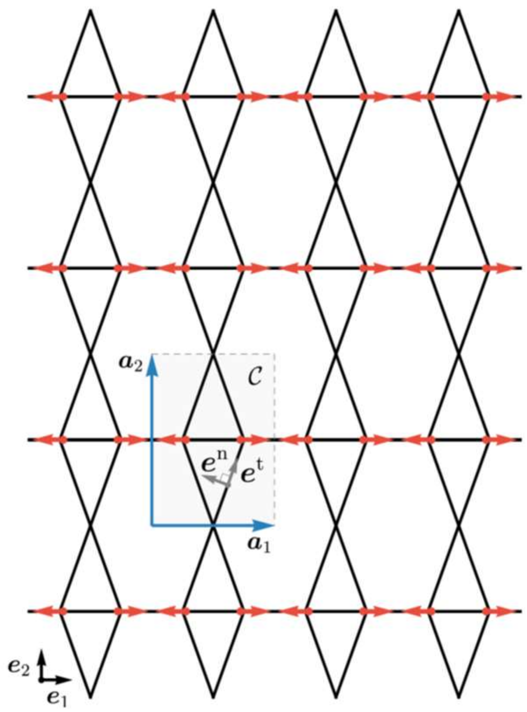

$\mathcal{B}_0$: Preloaded reference configuration

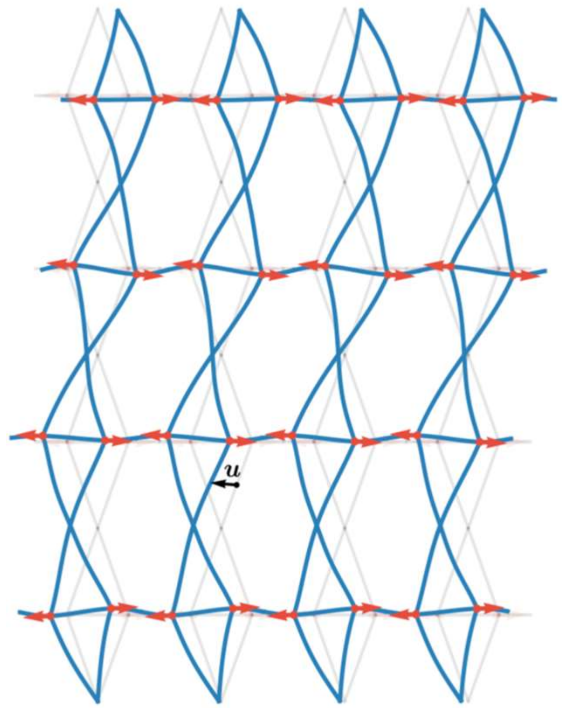

$\dot{\mathcal{B}}$: Incremental dynamic configuration

Flutter instability in the equivalent solid

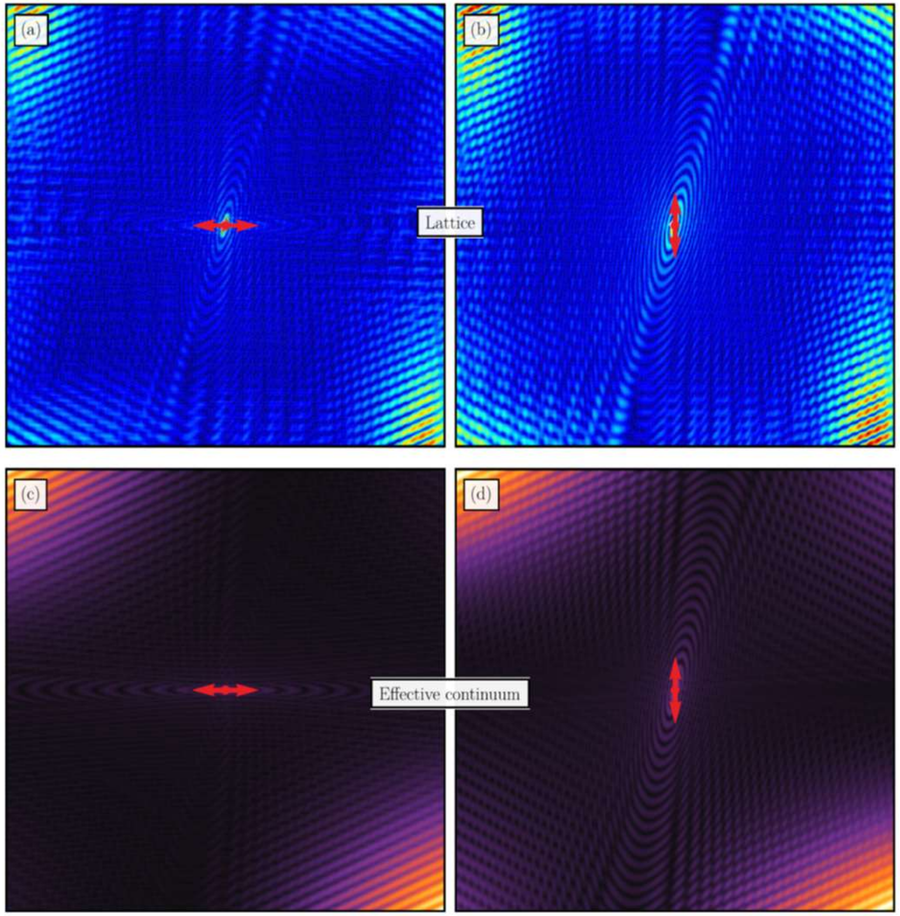

ERC Advanced Grant «Beyond»

Beyond hyperelasticity,
a new & unknown world of architected materials
to be explored and conquered

Flutter instability in solids and structures is reality!

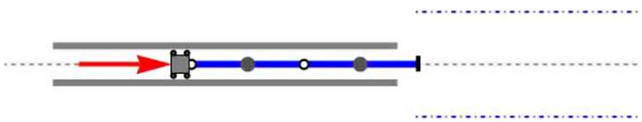

... Thanks for your attention!

Koutsogiannakis, P., Misseroni, D., Bigoni, D., Dal Corso, F. (2023) Stabilization against gravity and self-tuning of an elastic variable-length rod through an oscillating sliding sleeve. ***Journal of the Mechanics and Physics of Solids*** 181, 105452.

Rossi, M., Piccolroaz, A., Bigoni, D. (2023) Fusion of two stable elastic structures resulting in an unstable system. ***Journal of the Mechanics and Physics of Solids*** 173, 105201.

Bordiga, G., Piccolroaz, A., Bigoni, D. (2022) A way to hypo-elastic artificial materials without a strain potential and displaying flutter instability. ***Journal of the Mechanics and Physics of Solids*** 158, 104665.

Bordiga, G., Cabras, L., Piccolroaz, A., Bigoni, D. (2021) Dynamics of prestressed elastic lattices: Homogenization, instabilities, and strain localization. ***Journal of the Mechanics and Physics of Solids*** 146, 104198.

Cazzolli, A., Dal Corso, F., Bigoni, D. (2020) Non-holonomic constraints inducing flutter instability in structures under conservative loadings. ***Journal of the Mechanics and Physics of Solids*** 138, 103919.

Bigoni, D., Misseroni, D. (2020) Structures loaded with a force acting along a fixed straight line, or the "Reut's column" problem. ***Journal of the Mechanics and Physics of Solids*** 134, 103741.

Bigoni, D., Kirillov, O., Misseroni, D., Noselli, G.Tommasini, M. (2018) Flutter and divergence instability in the Pfluger column: Experimental evidence of the Ziegler destabilization paradox. ***Journal of the Mechanics and Physics of Solids*** 116, 99-116.

M. Tommasini, O. Kirillov, D. Misseroni, D. Bigoni (2016) The destabilizing effect of external damping: Singular flutter boundary for the Pfluger column with vanishing external dissipation ***Journal of the Mechanics and Physics of Solids*** 91, 204-215.

D. Bigoni and G. Noselli (2011) Experimental evidence of flutter and divergence instabilities induced by dry friction. ***Journal of the Mechanics and Physics of Solids*** 59, 2208-2226.